Tutorial. Surface EMG detection, conditioning and pre-processing: Best practices

R. Merletti*, G.L. Cerone

LISiN - Laboratory for Engineering of the Neuromuscular System, Department of Elctronics and Telecommunications - Politecnico di Torino, Turin, Italy

ABSTRACT

This tutorial is aimed primarily to non-engineers, using or planning to use surface electromyography (sEMG) as an assessment tool for muscle evaluation in the prevention, monitoring, assessment and rehabilitation fields. The main purpose is to explain basic concepts related to: (a) signal detection (electrodes, electrode–skin interface, noise, ECG and power line interference), (b) basic signal properties, such as amplitude and bandwidth, (c) parameters of the front-end amplifier (input impedance, noise, CMRR, bandwidth, etc.), (d) techniques for interference and artifact reduction, (e) signal filtering, (f) sampling and (g) A/D conversion, These concepts are addressed and discussed, with examples.

The second purpose is to outline best practices and provide general guidelines for proper signal detection, conditioning and A/D conversion, aimed to clinical operators and biomedical engineers. Issues related to the sEMG origin and to electrode size, interelectrode distance and location, have been discussed in a previous tutorial. Issues related to signal processing for information extraction will be discussed in a subsequent tutorial.

1. Introduction. Why are detection, amplification and conditioning important?

Among the main biomedical signals detected using surface electrodes (ECG, EEG and sEMG, carrying information about heart, brain and muscles, respectively), sEMG is the most complex and the least clinically applied. The information content of sEMG is remarkable and a very large number of publications, including textbooks and contributions to the J. Wiley and Elsevier Encyclopedias (Basmajian and De Luca, 1985; De Luca, 2006; Farina, 2006; Kamen and Gabriel, 2010; Barbero, Merletti and Rainoldi, 2012; Mitchell, 2016; Merletti and Farina, 2016), concern its extraction from the signal and its use in a wide range of applications (over 700 publications/year, over 100 review articles).

Contrary to ECG, the direct visual analysis of sEMG provides only information about on–off timing. The important information is obtained by computer processing which implies analog to digital (A/D) conversion of the signal. This, in turn, requires analog "signal conditioning" operations which consist in detection, amplification and filtering of the signal. These signal conditioning operations and the A/D conversion are the topics of this tutorial which is mainly aimed to non-engineers with a standard college background of mathematics. Clinical operators are the main target because it is fundamental for them to (a) collect the signal properly and distinguish a "good" signal from a "poor" one, (b) follow the evolution of the field, understand scientific papers and websites, and (c) be able to evaluate commercial claims and understand technical specifications of sEMG equipment in order to select and use it with proper knowledge of its performances and limitations.

Surface EMG applications are complementary to those of needle EMG (nEMG) in the areas of monitoring and assessing electrophysiological changes induced by training, physical therapy, rehabilitation, preventive, occupational and sport medicine, as well as in novel areas such as obstetrics, rehabilitation games and robotics (Mitchell, 2016; Barbero et al., 2012; Farina et al., 2013; Merletti, 2020; Merletti and Farina, 2016). The sEMG is a two-dimensional (2D) distribution of voltage in space evolving in time, like a movie [https://www.robertomerletti.it/en/emg/material/videos/f1/].

In the last two decades the rapid development of High Density Surface EMG (HDsEMG) and advanced multichannel sEMG processing for information extraction, has further increased the gap between the techniques available for research and their clinical applications (Campanini, 2020; Merletti, 2009, 2010a, 2010b).

---

* Corresponding author.
  E-mail address: roberto.merletti@formerfaculty.polito.it (R. Merletti).

Nomenclature

AP	Action potential generated by a single fiber and described in time or space
A/D	Analog to digital conversion
CV	Conduction velocity of the MUAPs
CMAP	Compound motor action potential (M-wave)
CMRR	Common mode rejection ratio
DC, AC	Direct current or voltage (continuous), Alternating current or voltage (sinewave)
DD	Double differential
DRL	Driven right leg
ECG	Electrocardiogram / Electrocardiography
EEG	Electroencephalogram / Electroencephalography
EMG, sEMG, nEMG	Electromyogram / Electromyography, Surface EMG, Needle EMG
SNR	Signal-to-Noise Ratio
IED	Inter-electrode distance (center to center)
MS	Movement scientist
MUAP	Motor unit action potential
M-wave	Motor-wave (CMAP)
NMJ	Neuromuscular junction
PLI	Power line interference
PSRR	Power supply rejection ratio
RMS	Root mean square value
RTI	Referred to input
SD, DD	Single differential, double differential
sEMG	Surface electromyogram or Surface electromyography
S/H	Sample and hold circuit

Technological advancements in the field of detection and conditioning of bioelectric signals are often recognized as technical, engineering-related, issues by users and operators. However, basic knowledge of detection and acquisition techniques, together with the most common related problems, is often required because: (1) the quality of signals strongly depends on how they are acquired by the user and by the understanding the user has of the acquisition-related problems; (2) the user is often a buyer and should be able to understand the technical specifications of the product; (3) in many clinical institutions the users are working with rehabilitation engineers and should be able to communicate with them.

Twenty years ago, a major European effort was carried out within the European Project "Surface Electromyography for Non-Invasive Assessment of Muscles" (SENIAM, www.seniam.org).

Dissemination of results was attempted through two main channels: the book on "European recommendations for surface electromyography" (Hermens et al., 2000) and the website www.seniam.org. A number of academic textbooks followed this effort with the goal of disseminating the rapidly advancing sEMG science and promoting its applications (Kamen and Gabriel, 2010; Barbero, Merletti and Rainoldi, 2012; Takada, 2012; Merletti and Farina, 2016). Efforts in this direction are continuing with a series of consensus and tutorial papers (Besomi et al., 2019; Merletti and Muceli, 2019).

More than 5000 peer reviewed articles, 160 review papers involving "sEMG", and 535 articles involving "sEMG applications" are listed in the Pubmed database. In the last thirty years, the rapid development of High-Density Surface EMG (HDsEMG) and advanced multichannel sEMG processing for information extraction (173 articles listed in the Pubmed database) increased the gap between the techniques available for neuromuscular investigation and their clinical applications. Simple, user friendly and inexpensive instrumentation became commercially available while the contribution of users to its development and applications has been limited by many "barriers" (Campanini, 2020). Tutorials and consensus papers, contributing to a deeper understanding of sEMG, are expected to help the potential sEMG users in approaching this field with proper guidelines for best practices.

The presentation of the topics in this tutorial, as in (Merletti and Muceli, 2019), is kept as simple as possible and requires only limited competences of the reader in electronics, signal processing and mathematics. Those who lack these competences can acquire them from on-line encyclopedias (De Luca, 2006; Farina, 2006; Merletti and Bonato, 2008; Merletti, Farina and Holobar, 2018; Merletti and Muceli, 2019) or free websites (Merletti, 2020).

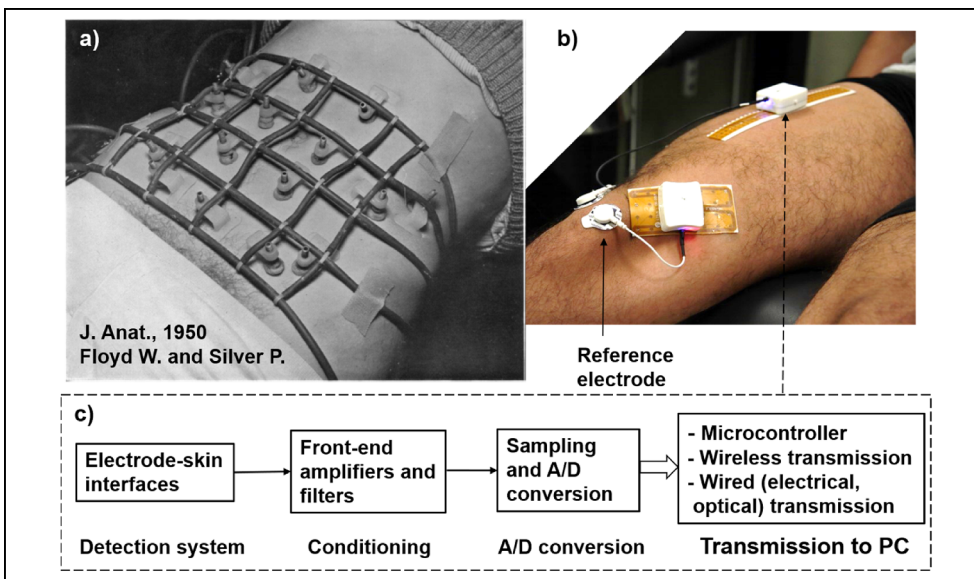Guidelines should not be considered as rigid rules but should be

Fig. 1. Surface EMG detection and conditioning. a) electrode system used by Floyd and Silver in 1950 (Floyd and Silver, 1950) to collect sEMG signals from the abdominal muscles, b) a modern wireless and user-friendly acquisition system with a 8x4 electrode array (up to four such systems can be used simultaneously on the same subject), c) block diagram of a general biomedical signal acquisition and transmission system, such as that depicted in panel b). Part a) is reproduced from (Floyd and Silver, 1950) with permission.

understood and correctly applied by the user depending on the purpose to be achieved. For example, when the user needs to extract information concerning simple events (e.g. activation/deactivation timing of a muscle), some requirement (e.g. noise, bandwidth) related to the sEMG conditioning system may be relaxed. On the contrary, situations where monitoring changes in sEMG during fatiguing contractions, or sEMG map features are desired, require the detection of high-quality sEMG signals with proper instrumentation. The researcher or the clinician must therefore understand and justify which choices are important for the intended purpose and which features of hardware and signal processing software are critical for such application. This multidisciplinary knowledge is rarely provided by the academic training of rehabilitation operators.

2. Block diagram of a sEMG signal detection and conditioning system.

The sEMG signal peak-to-peak amplitude on the skin ranges from a few tens of μV to 1–2 mV during a voluntary contraction and to about 5–6 mV in case of electrically elicited contractions (CMAP or M-wave). The signal is affected by noise and by a number of external sources of interference. Computer processing of the sEMG signal requires sampling in time and space (on the skin surface) and analog to digital (A/D) conversion. Since the input range of samplers and A/D converters is in the order of a few Volt, the signals must be amplified by a factor usually ranging from 100 to 2000 times. Analog filtering, to reduce noise and interference, is associated to amplification before the signal is sampled and A/D converted. Additional filtering and pre-processing may be applied to the digital version of the signal after the numerical signal is stored in a computer. This implies three processing blocks before the signal is transferred, in digital form, to a computer: (1) detection, by means of electrodes applied to the skin, (2) conditioning, by means of amplifiers and analog filters, and (3) sampling in time and A/D conversion.

Fig. 1 shows a sEMG acquisition system used by Floyd and Silver in 1950 (Floyd and Silver, 1950), a recent wireless system developed by Cerone et al (Cerone and Gazzoni, 2018; Cerone, Botter and Gazzoni, 2019), and the block diagram of the general bioelectric signal acquisition system contained in the white boxes, shown in Fig. 1c.

3. The electrode and the electrode–skin interface

Bioelectric signals are generated by ionic currents flowing into tissues and associated to specific physiological phenomena such as muscle (sEMG), heart (ECG), or brain (EEG) activity associated to the electrical activities of excitable tissues (e.g. neurons, skeletal muscle fibers, cardiac tissue). Electrodes are transducers detecting potential differences generated on the skin by ionic currents flowing in the body. It is important to underline that electrodes detect potential differences in the extracellular space and do not provide information about transmembrane currents. Surface electrodes are usually made with silver (Ag), or with a silver/silver-chloride (Ag/AgCl) sintered material and are applied on the skin's stratum corneum. This is the outermost layer of the epidermis, is 15–20 μm thick and strongly contributes to the electrode–skin impedance (see Section 3.3). The total skin thickness is about 1.2 mm (Yousef, Alhajj and Sharma, 2019). The electrode–skin contact may be mediated by conductive gel whose purpose is to fill air gaps between the metal and skin surfaces due to hair and irregularities and provide a stable electrode–skin interface.

The obstacle encountered by the electric charges (ions in the tissue

and gel, and electrons in the metal electrode) in flowing from the tissue to the amplifier inputs, through the electrode(s), is called electrode–skin impedance. In the case of bio-potential detection by means of surface electrodes, we have an electrode-gel and a gel-skin interface whose impedances will be in series with the skin impedance, dominated by the outermost layer of the skin, named "stratum corneum", that mainly consists of dead cells containing keratin (Lu et al., 2018), and form the electrode–skin impedance. This impedance depends on the gel composition, the skin treatment, the electrode material and size. Electrodes made of Ag or AgCl present an electrode–electrolyte impedance that is predominantly a resistance and is little affected by the frequency of the signal. These electrodes are indicated as "non-polarizable". Gold or gold-plated electrodes present an electrode–electrolyte impedance that is predominantly due to a capacitance and is therefore affected by the frequency of the signal (higher impedance values for low frequency signals). These electrodes are more resistant to corrosion and are indicated as "polarizable" because their impedance is frequency dependent. The first type is usually preferred because it reduces uncontrolled signal filtering at the electrode–skin interface (Bates and Chu, 1992; Cattarello and Merletti, 2016). Section 3.4 provides a more detailed analysis.

3.1. Filtering effect of a surface electrode

An electrically conductive electrode having area *A* "averages" the voltage distribution present under its surface and therefore provides a voltage that is a "smoothed" version of the evolving sEMG spatial distribution. The greater is *A* the greater is the smoothing and the "low-pass" filtering operation that attenuates or removes the high frequency components of the sEMG signal. Small electrodes (diameter < 3–5 mm) are therefore preferable to larger electrodes. For example, a circular electrode with diameter = 10 mm introduces a low-pass 3 dB corner frequency at 200 Hz (for muscle fiber conduction velocity of 4 m/s). This issue has been discussed in a previous tutorial (Merletti and Muceli, 2019). On the other hand, electrodes with a small surface have higher impedances that, if unequal, can lead to unacceptable power line interference, due to the so called "voltage divider effect", that will be discussed in Section 6.1 (see Fig. 11).

3.2. The electrode–skin junction as a generator of noise and DC voltage

Charge "carriers" are electrons in the metals and ions in the electrolytes (conductive gel and skin). At the interface with the metal electrode, there is a continuous exchange of charges between the metal carriers (electrons) and the electrolyte carriers (H^+, OH^-, Na^+, Cl^-, and many other ions) (Webster, 2013). This causes tiny random fluctuations of the voltage between the metal and the skin, which add to the sEMG signal as "noise". Additional noise is generated at the gel-skin interface. The root mean square (RMS) amplitude of this voltage noise, in the frequency band of 10–1000 Hz, is in the range of 1–5 μV_{RMS} depending on the electrode size, the electrode material, and the skin treatment applied (Godin, Parker and Scott, 1991; Fernández and Pallás-Areny, 2000; Huigen, Peper and Grimbergen, 2002; Koch, Schuettler and Stieglitz, 2002; Puurtinen et al., 2006; Piervirgili, Petracca and Merletti, 2014). This phenomenon currently posits a limit to the smallest sEMG signal that can be detected. This noise is averaged over the electrode surface and is therefore smaller for electrodes with larger surfaces, because of spatial low-pass filtering (Merletti and Muceli, 2019), as indicated in Fig. 2a. The electrode–skin junction also generates a slowly fluctuating voltage (up to about ± 200 mV), due to the half-cell DC

potential indicated as V_b in Fig. 2c (the other half being under the other electrode). This voltage should not cause "saturation" (Fig. 5c) of the front-end amplifier since such distortion could not be corrected by subsequent filtering.

Electronic amplifiers are also noise generators. Commercially available amplifiers for bioelectric signals conditioning introduce an input-equivalent noise voltage of 1–2 μV_{RMS} in the frequency bandwidth of 10–1000 Hz. Since the global noise level is mostly determined by the electrode–skin interface and not by the amplifier, expensive very low-noise amplifiers are currently not justified for sEMG applications.

3.3. The electrode–skin junction impedance

Impedance is the "obstacle" opposed by an electrical component to the flow of a sinusoidal current at a given frequency and is a function of such frequency. The tiny current flowing through the electrode leads to a voltage drop on the electrode–skin impedance which is different for each sEMG frequency component (harmonic). Non-polarizable Ag/AgCl electrodes can be modelled, in a first approximation, as circuit components having a mostly resistive impedance of about 40 kΩ cm^2 at 50 Hz, inversely related to the electrode surface (Fig. 2b). An "ideal" amplifier has an infinite "input impedance" and zero current flowing into it, but a "real" amplifier presents an input impedance. It is important to underline that the sEMG signal has many frequency components (or harmonics, as indicated in Section 5) and the input impedance is different for each of them. The impedance presented by the electrodes and amplifier at the power line frequency (50 Hz or 60 Hz) is the most important for reasons that will be discussed in Section 6.

Each electrode–skin contact can be modelled as an electrical impedance Z_e, which is a function of frequency, of electrode size (Fig. 2b) and of skin treatment (Fig. 3). This impedance cannot be measured directly because it is not possible to place a second "ideal" electrical contact below the skin, however we can measure the impedance between any two electrodes of a number of electrode pairs and estimate the individual electrode–skin impedances by means of a mathematical algorithm (Piervirgili, Petracca and Merletti, 2014). A simple model of this impedance is depicted in Fig. 2c. In general, the electrode–skin contact exhibits both resistive and reactive (capacitive) behaviour. Each electrode is connected to one input of a differential amplifier that should read its voltage without modifications, so that there would be no voltage drop on Z_{e1} and Z_{e2}. This implies that the amplifier front-end circuit must have a very high input impedance Z_i (see Sections 5.1 and 6.1) toward the amplifier's voltage reference (reference of its power supply).

The electrode–skin junction impedance and the input impedance of the amplifier (see: https://www.robertomerletti.it/en/emg/material/tech/) form a voltage divider with an attenuation factor $Z_i/(Z_i + Z_e)$ very close to 1 because $Z_e < < Z_i$ and can be neglected with respect to Z_i. As a consequence, the attenuation of the sEMG signal due to this voltage divider is negligible (Fig. 2d). The reason for having small electrode–skin impedances and large amplifier input impedances is explained in Section 6.1 and is relevant for the power line interference (PLI) rejection. The electrode–skin impedance usually decreases with time to 50–70% of its initial value in half an hour (Hewson et al., 2003; Piervirgili, Petracca and Merletti, 2014) possibly because of progressive sweat production or gel penetration into the skin pores.

3.4. Skin treatment

The skin is usually "treated", before electrode application, in the attempt to reduce the electrode–skin impedance and improve the stability and quality of the contact by removing dead cells and oily substances and reducing the thickness (and therefore the impedance) of the stratum corneum that acts as a capacitor. The most widespread skin treatment is rubbing with ethyl or isopropyl alcohol. Rubbing the skin with conductive abrasive paste is also a common procedure. "Stripping" the skin with pieces of adhesive tape (usually 5 clean pieces), to remove dead cells, is a less common procedure. The effects of these procedures have been investigated and compared (Piervirgili, Petracca and Merletti, 2014). Rubbing with abrasive paste followed by cleaning with a damp cloth, to remove the abrasive particles and residual paste, provides lower values of electrode–skin noise and much lower values of electrode–skin impedance than other treatments, as depicted in Fig. 3. Skin abrasion also reduces the amplitude of motion artifacts (Tam and Webster, 1977; Burbank and Webster, 1978; Webster, 1984).

Fig. 3 shows that rubbing the skin with alcohol is not effective for reducing electrode–skin impedance and noise. Rubbing with abrasive paste is much more effective and reduces electrode impedance, noise, and impedance unbalance much more that alcohol.

3.5. Special electrodes

In addition to the classical adhesive individual electrodes or multi-electrode arrays (Fig. 1b) other types of electrodes are available or being developed. They are based on capacitive coupling, on tattoo-like or skin-printed conductive inks, and on surfaces with many micro-pins that perforate the stratum corneum. They are briefly mentioned here because they are currently available in research labs but may soon be on the market.

- Capacitive electrodes have metal surfaces isolated from the skin by a thin insulating layer and the signal is transferred by electric induction (leading to displacement currents). They do not require conductive paste or skin treatment but are very sensitive to motion artifacts and to external interferences and need electrical shielding (Merletti, 2010; Spinelli et al., 2016).
- Skin-printed electrode offer exciting opportunities for long-term electrophysiology monitoring. They provide stable and repetitive recordings at both a hospital environment and a home setting.
- Temporary-tattoo dry electrode systems for sleep analysis have been tested successfully (Zucca et al., 2015; Bareket et al., 2016; Shustak et al., 2019).
- Individual electrodes or multichannel electrode arrays for HDsEMG may consist of small sharp pins that perforate the stratum corneum and penetrate into the skin for 0.2–0.5 mm. They provide positional stability (with respect to the skin) and are still in the experimental phase (Griss et al., 2002; Kim et al., 2018).
- Individual or multichannel electrodes can be printed on fabric and integrated into clothes (Gazzoni, 2015; Pani et al., 2019). They are indicated for long-term or outdoor applications
- Special acoustically-matched hydrogel electrodes allowing the simultaneous acquisition of sEMG signals and ultrasound (US) images (eliminating the shadow artifact produced by the electrodes on the US images) have been recently developed by Botter et al. (Botter et al., 2019).
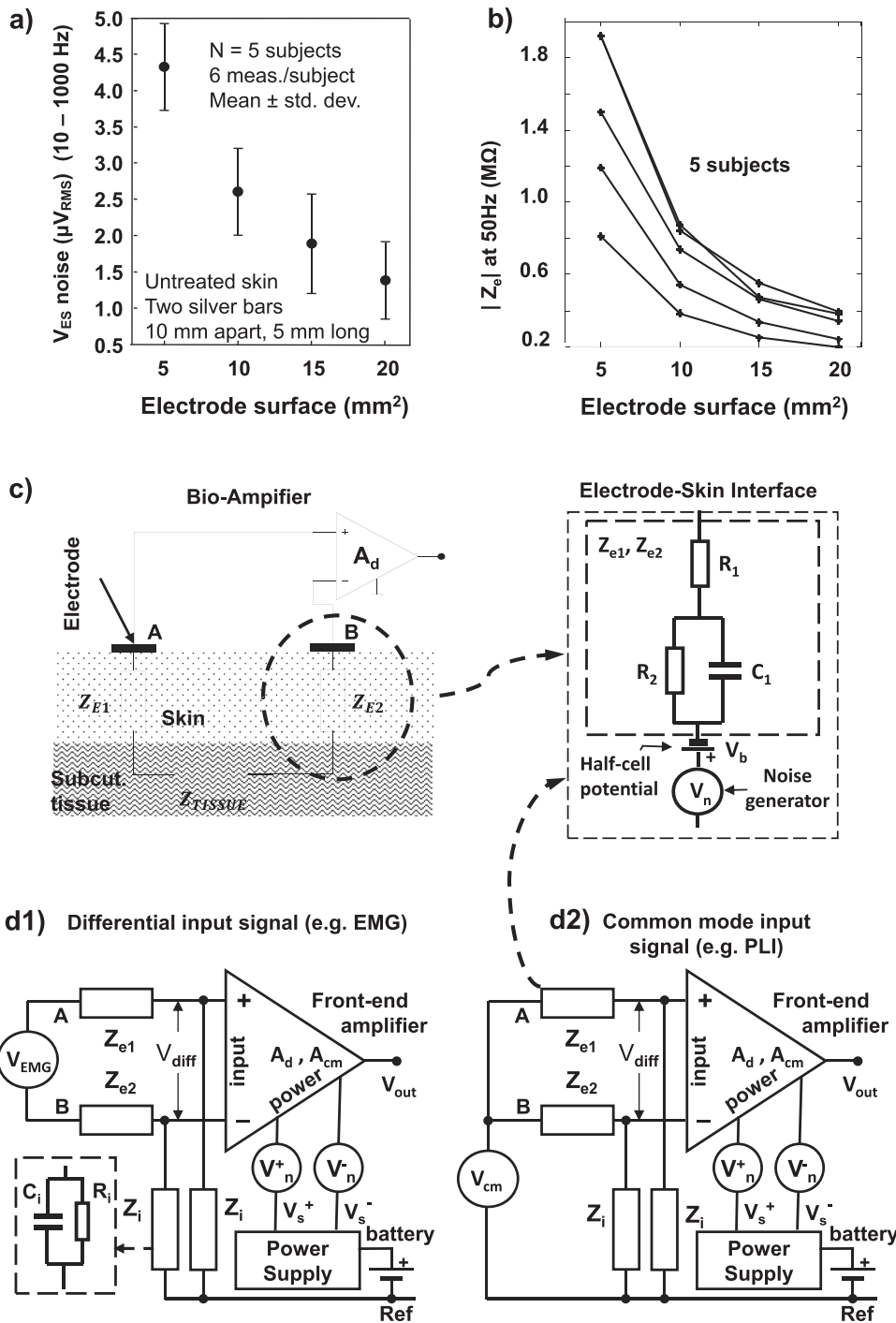
Fig. 2. Electrode-skin impedance and noise. a) RMS value of the noise detected between pairs of gelled Ag-AgCl electrodes of different area applied to the untreated skin of a relaxed biceps brachii b) magnitude of the impedance of one electrode–skin interface measured on five subjects using electrodes of different areas applied to a relaxed biceps brachii, c) model of the electrode–skin contact including impedance, half-cell potential and noise generator. d) model of the front-end amplifier used to detect EMG signals. Differential (e.g EMG) and Common mode (e.g. Power Line Interference) input signals are shown in d1) and d2) respectively. The triangle indicates the front-end amplifier, which amplifies the common mode voltage by a factor A_{cm} and the differential voltage by a factor A_d. Problems related to the detection of unwanted common mode signals will be discussed in Section 6. The amplifier has two input terminals and two power supply terminals. Circles indicate sources of signal, interference or noise. In panel c) the impedance Z_e is mostly due to C_1 for polarizable electrodes (Au) and to R_1 and R_2 for non-polarizable electrodes (Ag-AgCl). Panels a) and b) are reproduced, with permission, from Fig. 3.6 and 3.7 of (R. Merletti and Farina, 2016) .
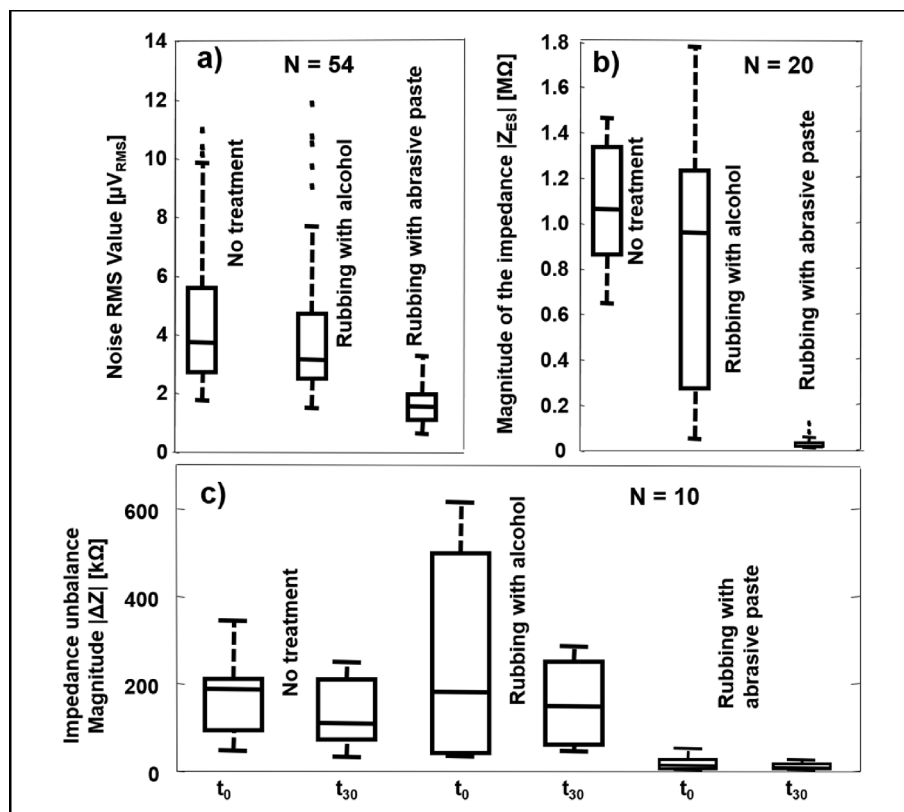
Fig. 3. Electrode-skin impedance and noise for three skin preparation conditions. Electrodes are silver surfaces (1x5 mm, IED = 10 mm) with gel, placed on the dominant biceps brachii. Whiskers plots show median, first and third quartile, range and outliers. a) RMS of the noise between two electrodes (6 electrode pairs from each of 9 subjects), b) magnitude of the impedance of a single electrode–skin contact at 50 Hz. N = 20 (two measurements on each of 10 subjects), c) magnitude of the impedance unbalance $|\Delta Z|$ between two electrodes with gel (1x5 mm, IED = 10 mm), N = 10). Measurements made at t_0 and 30 min later (t_{30}). Data are redrawn from Figs. 4 and 5 of (Piervirgili, Petracca and Merletti, 2014), with permission.

4. Common mode signals and artifacts.

4.1. Common mode signals

Common-mode signals are identically present on both inputs of a differential amplifier and, of course, on the inputs of an array of monopolar amplifiers. They are measured with respect to the amplifier voltage reference and their source may be endogenous (inside the body) or exogenous (outside the body). It is important to reject common mode signals that otherwise will overlap to the sEMG signal of interest. The most frequent endogenous common mode source is the ECG signal that can be detected on neck, chest, back, and abdominal muscles. End-of-fiber effects and EMG generated by remote muscles contribute to common mode as well as to differential voltages (Figs. 6 and 8 of (Merletti and Muceli, 2019)). The most common exogenous source is the interference due to the electric induction (capacitive) coupling between the power line and the subject-amplifier system. Also, nearby equipment generating electric or magnetic fields at 50 Hz or 60 Hz can cause power line interference (PLI) whose reduction techniques will be discussed in Section 6.

Very often, amplifiers integrated into a battery-powered system require two symmetric voltages to operate (dual power supply). The power supply voltages (V_s^+ and V_s^- in Fig. 2d) may be provided by a DC/DC converter which converts the single supply battery voltage into a dual supply voltage. The power supply DC voltages of the front-end amplifier, V_s^+ and V_s^- in Fig. 2d, may be affected by noise characterized by spikes or high frequency "ripples" indicated as V_n^+ and V_n^- (Fig. 2d) as described in Section 5.1. Their effect on the detected signal is defined by the Power Supply Rejection Ratio (PSRR) capability of the amplifier. When sampled, this "noise" may appear on all channels. The same effect may be due to some transient in the volume conductor affecting groups of channels in a highly correlated way, as indicated in Fig. 4 and observed by Turner and Russo (Turner et al., 1995; Russo and Merletti, 2017). This phenomenon requires further investigation.

Additional sources of interference are neon lights (Winter and Webster, 1983a) and other devices (e.g. LED lights, medical equipment, computers and laptops). Other apparent "disturbances" are due to the input/output saturation of the amplifier whose output voltage cannot exceed V_s^+ and V_s^- (Fig. 2d and Fig. 5c). Fig. 5a, 5b and 5c show examples of signal under-amplified (A_d = 500), correctly amplified (A_d = 2000), and over-amplified (A_d = 10000) considering an amplifier voltage range of ± 12 V. Saturation of the amplifier is evident in the third case and the highly distorted signal may be misinterpreted as an external disturbance. Fig. 5d shows a transient event (e.g. due to motion artifacts), in one monopolar channel. Such event will appear with opposite polarities in two single differential channels (SD), as shown in Fig. 5e, and could be misinterpreted as sEMG (Jahanmiri-Nezhad et al., 2015). The upper trace in Fig. 5f shows a sEMG channel strongly affected by the ECG signal. Since the ECG spectrum overlaps the sEMG spectrum, filtering cannot be used to remove the ECG. In this case specific algorithms identify the shape and the timing of the ECG artifact and subtract it from the sEMG recording. The lower trace of Fig. 5f shows the result. Another option to reduce ECG artifacts during monopolar HDsEMG acquisition is to place, when possible, the reference electrode near the exploring electrodes (but not on active muscles) in order to reduce the detection volume of possible common mode sources.
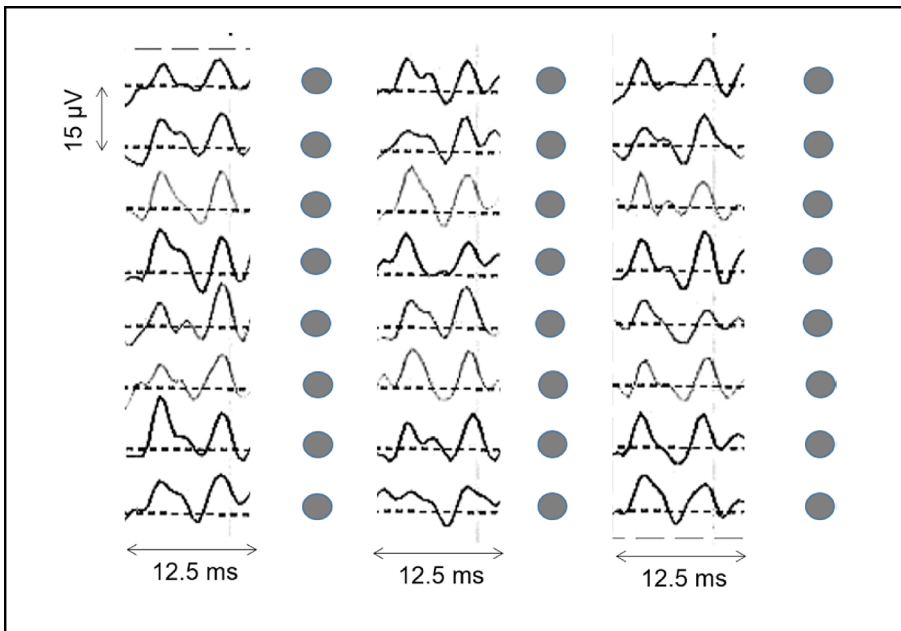
Fig. 4. Example of highly correlated noise across the monopolar channels of an 8x3 electrode grid applied on a piece of pig skin to avoid any sEMG contribution. This noise is reduced but not cancelled by the differential detection. Interelectrode distance = 10 mm in both directions, electrode diameter = 3 mm. Modified from (Russo and Merletti, 2017).
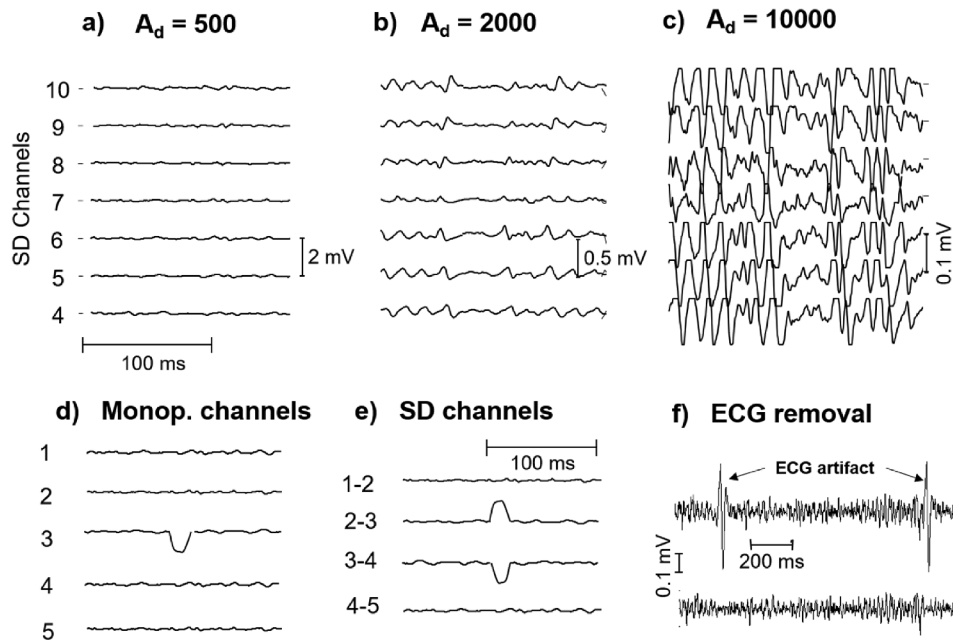

Fig. 5. Examples of apparent and real artifacts. a) low amplifier gain does not allow visualization of sEMG, b) amplifier gain about right: MUAPs are evident, c) amplifier gain too high; the sEMG peaks saturate the amplifier and may be interpreted as artifacts or external disturbances, d) and e) a transient on one monopolar channel results in the same transient on two SD channels with opposite polarity, f) example of ECG artifact removed by suitable software. In a), b) and c) the outputs have the same scale: the indicated scale is the output scale divided by Ad to refer it to the input. See text for details (Courtesy of A. Gallina, C. Ritzel, and T. Vieira).

4.2. Motion artifacts

Other disturbances derive from small movement of the electrodes with respect to the skin causing momentary loss of contact or fluctuations of the DC voltage due to the charges accumulated at the interface (half-cell potential V_b in Fig. 2c). Sources of motion artifact are: cable motion, electrode–skin contact movements, stress applied to the skin underlying the electrodes (De Talhouet and Webster, 1996). To limit motion artifacts, electrodes must be light and well fixed and cables to the amplifier must be short, but not in tension, and tied to the skin. Active electrode systems that incorporate the electrodes and the

amplifiers (and often include the transmitter for wireless data transfer, as in Fig. 1b) eliminate the cable problems but must be light to limit the increase of the mass of the system and, therefore, the inertial forces acting on the interface during movement.

Fig. 6a shows the results of manually shaking the cable connecting a 16-electrode linear array to an array of 15 differential amplifiers. The amplitude spectrum (that is the magnitude of the Fourier transform of the signal) of one SD channel for the three cases shown in Fig. 6a is depicted in Fig. 6b. It is clear that a high-pass filter will reduce the contribution of this artifact to the signal. The selection of its cut-off frequency f_c is a compromise between the intensity of the artifact and
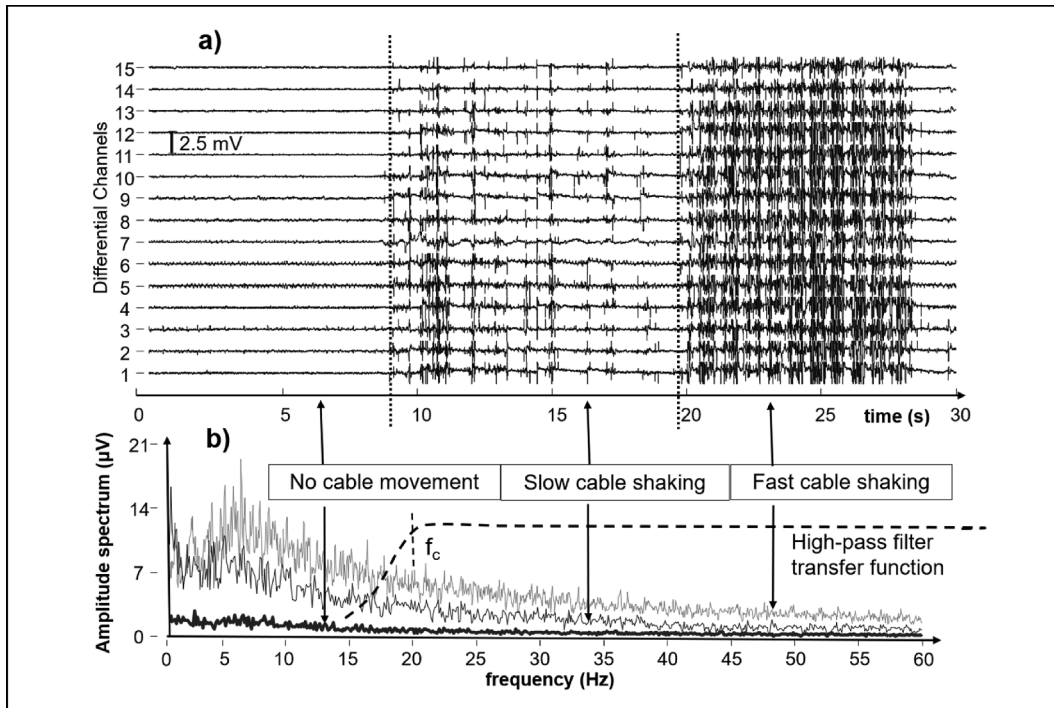
Fig. 6. Artifacts caused by manually shaking the cables connecting the electrodes to the amplifiers. a) differential recordings from a linear array of 16 electrodes spaced 10 mm apart, three levels of shaking, b) amplitude spectra (magnitude of the Fourier transform) of one SD channel in the three conditions. The spectra of the artifacts have a long tail that is not removed by high-pass filtering, even with a cut-off frequency f_c = 20 Hz (Courtesy of A. Gallina, C. Ritzel, and T. Vieira).
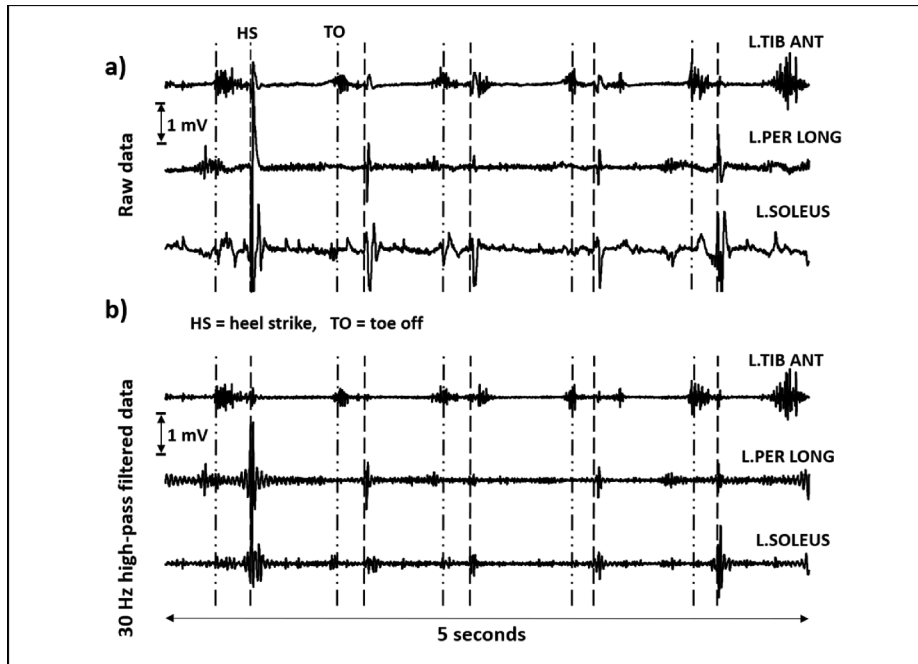

Fig. 7. Effect of filtering on original sEMG signals detected from the left tibialis anterior, peroneus longus and soleus muscles during walking of a child with cerebral palsy. a) original signals, b) signals filtered with a bidirectional 4th order high pass filter with cut-off frequency of 30 Hz (see Section 5.2). HS = heel strike, TO = toe off. Note the residual high frequency oscillations near the artifact spikes due to the high frequency components of the artifacts remaining after filtering. Reproduced, with permission, from (Merlo and Campanini, 2016).

the attenuation of the sEMG signal in the low frequency spectral region (see section 5). A detailed analysis of this problem has been presented in (De Luca et al., 2010).

Fig. 7a shows the original sEMG detected from the left tibialis anterior, peroneus longus and soleus muscles during gait of a child with cerebral palsy. Movement artifacts associated to the heel strike (HS) are evident. Fig. 7b shows the same signals after application of a fourth order bidirectional high pass filter (see Section 5.2) with cut-off frequency of 30 Hz. Once filtered, the residual high frequency components

of the artifacts can no longer be recognized as such by a naïve user and may be misinterpreted as sEMG or reflex activity and even be medically treated (Merlo and Campanini, 2016).

5. Surface EMG conditioning systems.

Amplitude, properties of the power spectrum, or other features (such as muscle fiber conduction velocity, signal entropy, etc) may be of interest and can be obtained in different ways, as will be discussed in

detail in subsequent tutorials. Their estimation requires proper signal conditioning. Amplification is required to match the A/D converter input range (typically 3 V to 10 V) and filtering is needed to reduce high frequency noise and low frequency movement artifacts.

This Section describes the basic principles, features and problems related to the amplifying and conditioning circuits. The amplifying and conditioning block is an analog circuit having three main functions: (a) amplify the input signal in order to adapt the amplitude range of the signal to that of the A/D converter system, (b) filter out the harmonics of the input signal outside the frequency bandwidth of the sEMG, (c) reject the common mode noise and interference sources inside the frequency band of the signal (e.g. the common mode voltages at the input of the acquisition system caused by the capacitive coupling between the subject and the power line).

5.1. The front-end amplifier: Main features and parameters

The acquisition of biopotentials requires an analog system composed by electrodes, amplifiers and filters. The amplifier is an analog electronic circuit usually comprising a differential amplifier ("front-end" circuit) and a series of single-ended stages used to further amplify and filter the signal of interest. Monopolar signals, measured between each electrode and a common reference, are also often acquired. In this case, one input of the differential amplifier is connected to such reference electrode.

The "differential" (or bipolar, or Single Differential – SD) detection is useful because unwanted common mode input signals (V_{cm} in Fig. 2d), such as the power line interference (PLI), are theoretically cancelled at the detection point. Alternatively, monopolar signals may be acquired, and SD signals may be computed as the difference between two channels after A/D conversion. This approach implies a verification that saturation due to PLI is not taking place in the analog system before the A/D conversion. Saturation is indicated by flat segments at the top and/or bottom of the signal (Fig. 5c).

It is important to note that the voltage at each input of the analog front-end amplifier is referred to a common voltage reference level (Fig. 2d). This is the reason why, a differential sEMG amplifier has a third electrode, named "reference electrode", that must be placed on an electrically non active region on the subject (usually a bone prominence not near the muscle(s) of interest). Today, two-electrode amplifiers (i.e. amplifiers that do not need a physical reference electrode) have been

developed (Dobrev and Daskalov, 2002; Dobrev, Neycheva and Mudrov, 2005; Spinelli and Mayosky, 2005) and are commercially available. They do not eliminate the need for a reference voltage but generate it internally.

There are some important (and often critical) features of the front-end amplifier that a clinical user should be aware of. They are the input impedance (Z_i), the differential and common mode amplifications (A_d and A_c) and the associated common mode rejection ratio (CMRR), the power supply rejection ratio (PSRR), the input voltage and current noise levels. These features are defined below.

Input impedance. The differential input stage of the front-end amplifier presents an internal impedance Z_i between each input and the reference which can be modelled as a large resistance R_i (order of 1 GΩ −10 GΩ) in parallel with an unwanted but unavoidable capacitance (i.e. parasitic capacitance) C_i (order of 2 pF-20 pF). Because of this capacitance the input impedance is different for different frequency components of the input signal. For clarity, in Fig. 2d, Z_i is drawn outside the amplifier and modelled as an ideal component but is actually inside it. The magnitude of the internal impedance for a given frequency f is given by:

$$|Z_i(f)| = \frac{R_i}{\sqrt{1 + (2\pi f R_i C_i)^2}} \qquad (1)$$

where R_i and C_i are respectively the input resistance and capacitance of the front-end amplifier (Fig. 2d) and f is the frequency of each harmonic of the signal of interest. Considering the model of Fig. 2d, in the frequency band of the sEMG the input current flows predominantly in C_i (that is, the term $(2\pi f R_i C_i)^2$ is much greater than 1 and Eq. (1) simplifies to $|Z_i(f)| \simeq 1/2\pi f C_i$ which is the impedance of C_i). In fact, in the sEMG frequency range (10–500 Hz), the impedance presented by the input capacitance C_i is in the range of 20–800 MΩ, depending on the value of C_i, that is usually much lower than that presented by the resistance R_i of modern amplifiers (5000–10000 MΩ). For reasons that will be explained in Section 6, it is important to know the amplifier's input impedance at the power line frequency (50 Hz or 60 Hz). This impedance is of the order of a few hundred MΩ and is mostly determined by the input capacitance of the amplifier, **not** by its input resistance. It is therefore misleading to report only the input resistance in the technical specifications of sEMG amplifiers. Manufacturers should report the input impedance at 50 Hz or the input resistance and the input capacitance that is in parallel with it. In this case, the magnitude of the input
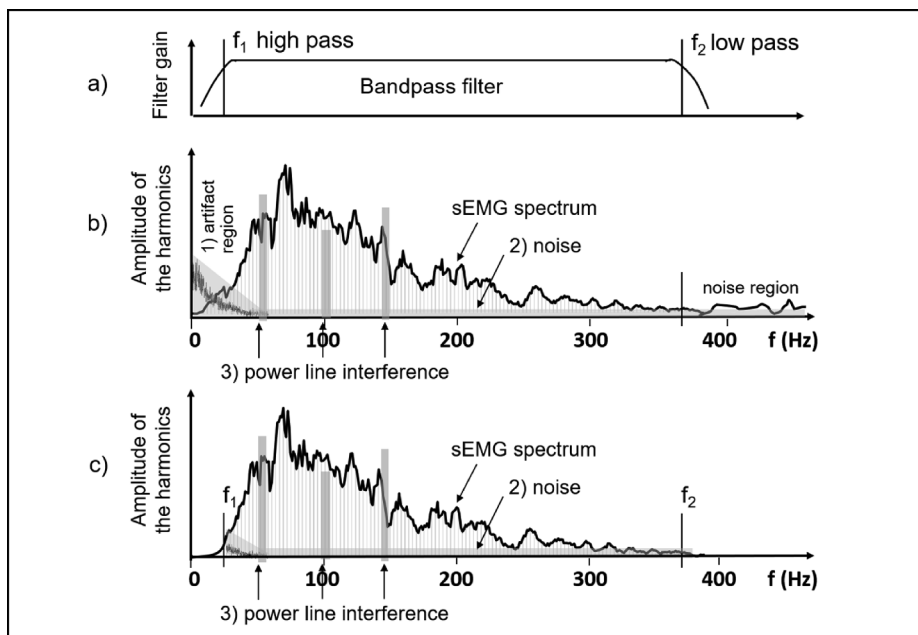

Fig. 8. Example of band-pass filtering of the amplitude spectrum of the sEMG signal. a) plot of the filter gain versus frequency, b) sEMG amplitude spectrum. The gray regions indicate the spectra of noise, artifact, and power line interference. Low frequency contributions (1) are mostly due to artifacts (see Fig. 6). Background noise (2) is mostly due to the electrode–skin interface. c) sEMG amplitude spectrum after band-pass filtering. The first three harmonics of power line interference (3) are indicated; more or fewer than three lines may be present (see Fig. 13). The vertical hatching represents the harmonics of the signal. The cut-off frequency of the low pass filter defines the maximal frequency of the signal that is important for defining the lowest possible sampling frequency required to avoid "aliasing" (see Section 7).
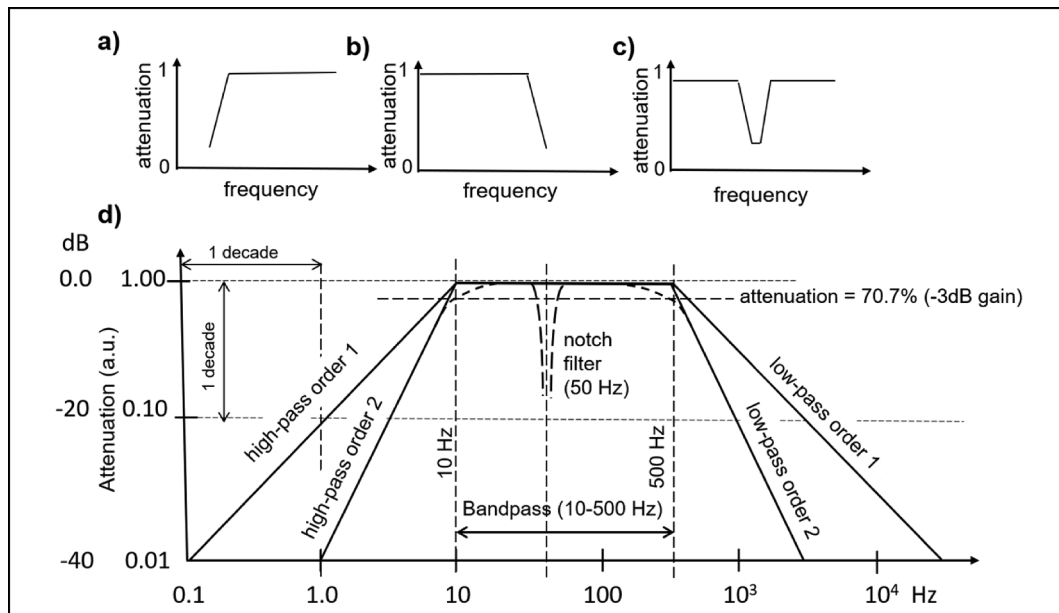
Fig. 9. Transfer function of analog or digital filters used for sEMG conditioning. a) high pass flter, b) low-pass filter, c) notch filter, d) combination of filters and concept of filter order. Note the logarithmic scales on both axes. A notch filer removes spectral lines of an undesired interference as well as spectral line of the sEMG signal that may be important See text for further explanation.

impedance of the front-end amplifier can be calculated using Eq. (1) with f = 50 Hz or 60 Hz.

Differential and common mode amplifications. Consider the circuit depicted in Fig. 2d and assume $V_{diff} = 0$. The common mode voltage V_{cm} is then applied to both terminals A and B. This voltage will be amplified (actually it will be attenuated) by the common mode amplification A_{cm} ($A_{cm} \ll 1$). The differential voltage V_{diff}, when present, will be amplified A_d times and the total output voltage will be

$$V_{out} = V_{cm}A_{cm} + V_{diff}A_d \qquad (2)$$

A "good" amplifier should have a very small A_{cm} value ($A_{cm} \ll 1$) and a ratio A_d/A_{cm} of at least 10^4 to 10^5. A_d/A_{cm} is the common mode rejection ratio (CMRR) and describes the capability of the differential amplifier to reject or attenuate common mode signals (such as PLI) applied at the input of the differential amplifier. Its value depends on the frequency of the input signals V_{cm} and V_{diff} and is usually expressed in deciBels (dB) as $20log_{10}(A_d/A_{cm})$. Its value is particularly important at the power line frequency (see Section 6). Acceptable values are in the range 90–110 dB at 50–60 Hz. Consider that V_{cm} may be in the order of V while V_{diff} is in the order of a few mV.

PSRR (Power Supply Rejection Ratio): Front-end amplifiers are powered by a DC power supply providing the $V_s{}^+$ and $V_s{}^-$ voltages showed in Fig. 2d, that define the maximum output voltage range of the detected signals (Fig. 5c). DC/DC converters are often used to produce these two voltages. These devices often produce high frequency spikes that appear at the output of the amplifier. The capability of the front-end amplifier to reject fluctuations of the power supply voltage is measured by the PSRR parameter. This capability is measured in dB and is near 60 dB which means that 0.1% of the voltages $V_n{}^+$ and $V_n{}^-$ (Fig. 2d) contributes to the input voltage of the front-end amplifier.

Noise. A front-end amplifier is a generator of electronic noise. This means that, when the input terminals are connected together and to the reference ($V_{cm} = V_{diff} = 0$), the output voltage is not zero and looks like a small random signal. If this output signal is divided by A_{diff} the result is called the "equivalent input voltage noise" or "referred to input (RTI) noise" which is the input noise voltage that would produce the observed output in an ideal noiseless amplifier. Together with the noise generated at the electrode–skin interface, this noise posits a limit to the smallest sEMG signal that can be detected. Noise is measured as RMS

voltage in a certain frequency range (e.g. 1 μV_{RMS} in the sEMG bandwidth of 20–500 Hz) or is characterized by its power spectral density (V^2/Hz). The noise signal is typically considered as added to the signal of interest, it is different from interference (e.g. ECG, PLI) and should not be confused with interferences or crosstalk.

5.2. Analog low-pass, high-pass and notch filters

The analog conditioning system has the purpose of amplifying the sEMG while reducing the contributions of artifacts, noise and power line interference (see Section 6), before the signal is converted in a sequence of binary numbers by the A/D converter. Additional attenuation of undesired contributions may be achieved by digital processing after the A/D conversion. The sampling operation (Section 7) requires that the signal is "band-limited". For this reason it should have no or negligible frequency components (harmonics) above its "maximal frequency" indicated with f_2 in Fig. 8. The users of sEMG acquisition systems should be familiar with the basic notions and parameters, related to the concept of signal filtering, presented below.

The term "filtering" refers to the attenuation of specific harmonics of the signals that are outside (occasionally inside) the bandwidth of interest. The "harmonics" or "frequency components" or "spectral lines" of a signal are the sinusoidal components into which a signal can be decomposed by the Fourier analysis and whose sum reproduces the signal. Readers unfamiliar with these concepts are referred to more elementary material available at (Merletti, 2020).

The bandwidth of a signal is the range of frequency components (harmonics) the sum of which makes up the signal. The amplitude (or power) spectrum of the signal is the plot of amplitude (or power) of the harmonics of the signal versus frequency. Fig. 8b shows the typical amplitude spectrum of a sEMG signal. The gray areas represent undesired contributions; the low frequency artifacts (see Fig. 6), the background random noise and three harmonics of the power line frequency (at 50, 100 and 150 Hz). Low frequency artifact noise can be reduced by a high-pass filter with cut-off frequency in the range of 10–30 Hz and high frequency noise can be reduced with a low-pass filter with cut-off frequency in the range of 350–400 Hz, as indicated in Fig. 8a. Since also some sEMG harmonics are reduced by these filters, the choice of the specific cut-off frequencies is a compromise (see
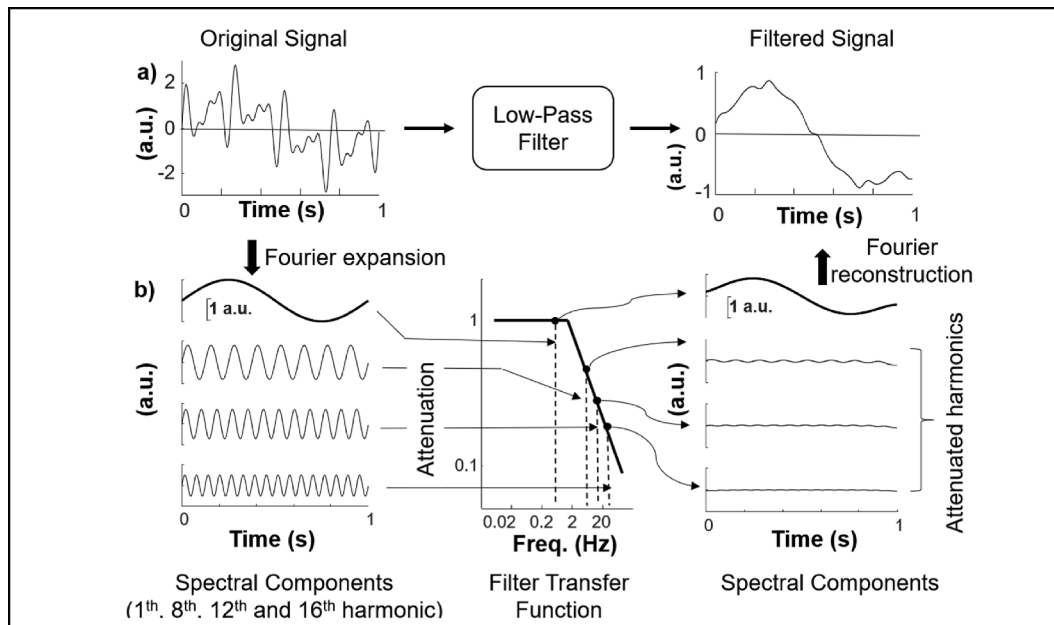
Fig. 10. Operation of a low-pass filter. a) examples of input and output signals of the filter, b) harmonics of the input and output signals of the filter undergoing different attenuations. See text for details.

Section 8). The PLI can be attenuated by an analog notch filter at 50 Hz. Other harmonics of the power line may be present, and their attenuation requires more sophisticated numerical algorithms (Section 6.2). The "transfer function" of a filter is the plot of the attenuation or amplification (gain) applied by the filter to the harmonics of the signal versus the frequency of such harmonics, as indicated in Figs. 8a and 9.

Order of a filter. The transition from the passed band to the attenuated band of a filter may be more or less sharp. This sharpness is indicated by the order of the filter. Fig. 9d shows the transfer function of low-pass and high-pass filters of order 1 and 2. Note the logarithmic scales along both axis where the ticks indicate decades. A low-pass /(high-pass) filter of order 1 reduces the amplitude of the harmonics of the input signal by a factor 10 (20 dB/decade) when the frequency is one decade above/(below) the cutoff frequency. A filter of order 2 reduces the amplitude of the harmonics of the input signal by a factor 100 (40 dB/decade) when the frequency is one decade above/(below) the cutoff frequency. The same applies to a band-pass or to a notch (band-reject) filter. The transition from the pass-band to the attenuated-band region is smooth and there is no sharp corner. By convention, the cut-off frequency of a filter is defined as the frequency at which the amplitude of the corresponding harmonic is reduced to 70.7% (its power is reduced to 50%). Analog filters used for conditioning the sEMG signal are usually of order 1 or 2. Digital filters may easily be of order 4, 6 or 8.

Operation of a filter. Fig. 10 shows the operation of a low-pass filter. The signal applied to the filter (left panel of Fig. 10a) contains many harmonics. Let us consider the 1st at 1 Hz (of interest), the 8th, 12th and 16th (among those to be reduced by the filter). The filter transfer function indicated in the central panel of Fig. 10b attenuates them as indicated in the right panel. They form the new signal indicated in the right panel of Fig. 10a which is the result of the filtering operation. The same sequence of operations is performed by a high pass filter. This sequence of operations may be performed by an analog filter (made by electronic components) or by a numerical (digital) filter, implemented in software by mathematical manipulation of samples.

For reasons whose explanation exceeds the purpose of this tutorial, a low pass filter introduces a signal delay which may be undesirable. Specific digital filters (not analog ones), applied off-line, can avoid this problem: they are called "non-causal" or "bidirectional". They filter the signal twice, first starting from the first sample and then again but backward, starting from the last sample, therefore compensating the

introduced delays. There are filter families with slightly different performances. The Chebyshev filter has the best approximation to the ideal response, the Butterworth filter has a maximally flat frequency response, the Bessel filter, has an optimal phase delay. Their description exceeds the purpose of this tutorial. Additional information can be found in (Winder, 2002).

Notch filters. In some simple sEMG equipment, analog notch filters are incorporated in the signal conditioning block to reduce PLI. An example is provided in Fig. 9d. They alter the features of the sEMG and are acceptable only for simple applications such as biofeedback. In addition, they attenuate only the first harmonic of the interference (50 Hz or 60 Hz). They should not be used if any subsequent sEMG processing or estimation of sEMG features are planned. More sophisticated and effective ways for reducing power line interference are described in Section 6.

6. Reduction of power line interference

One of the main problems affecting the detection of ECG, EEG and sEMG is the susceptibility of the acquisition system to 50 Hz/60 Hz PLI. This susceptibility is mainly due to the stray capacitive coupling between a subject and the power line source (220 V_{RMS} at 50 Hz or 110 V_{RMS} at 60 Hz).

Fig. 11 shows the capacitive couplings between a subject, the active wire of the power line source (C_1) and the power line ground (C_2). C_1 and C_2 form a capacitive voltage divider of which the human body is a node. Stray coupling with the power line and ground, due to the capacitances C_1 and C_2, creates a common mode voltage V_{cm} (Fig. 2d, Fig. 11 and Fig. 12a) and small currents in the body, of the order of nA, indicated as I_{AC}, flowing through the voltage divider.

The common mode voltage present at the input of the electrode-amplifier system depends on the capacitive voltage divider described above and on the value of the electrode–skin impedance of the reference electrode. The power line interference, due to this common mode voltage can be reduced at the source using particular strategies, or can be reduced, after signal acquisition, by digital processing. Both techniques are described in the following subsections.
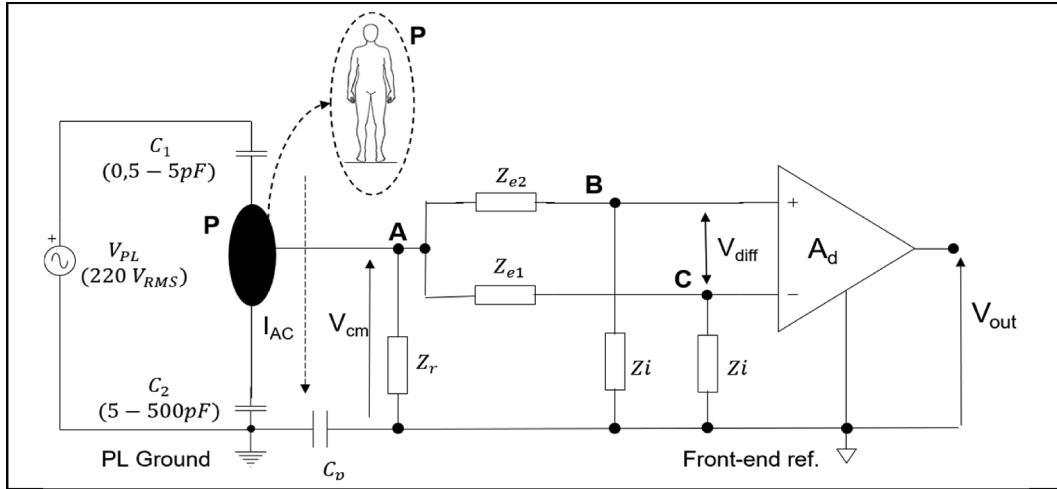
Fig. 11. Equivalent circuit showing the common mode input voltage of a front-end amplifier. The circuit includes the capacitive coupling between the power line and a subject connected to the amplifier. The capacitor C_p represents the isolation capacitance between the amplifier reference and the ground. Z_{e1}, Z_{e2}, and Z_r are the impedances of the electrode–skin interfaces and of the reference electrode respectively. The body of the subject is assumed to be equipotential, for the PLI, at the voltage between A and PL Ground.

6.1. Reduction of power line interference at the source

6.1.1. Matching electrode impedances and reducing the input common mode voltage

Consider the front-end amplifier, depicted in Fig. 2d and Fig. 11, with shorted inputs and only the common mode voltage present between A and the reference.

Consider the two voltage dividers made by Z_{e1} and Z_i and by Z_{e2} and Z_i, where Z_{e1} and Z_{e2} are the electrode–skin impedances and Z_i is the input impedance of the amplifier. The voltages in B and C are, respectively $V_B = V_{cm} Z_i/(Z_i + Z_{e2})$ and $V_C = V_{cm} Z_i/(Z_i + Z_{e1})$.

The differential voltage $V_{diff} = V_B - V_C = V_{BC}$ present at the input of the amplifier is approximately $V_{diff} = V_{cm} (Z_{e2} - Z_{e1})/ Z_i = V_{cm} \Delta Z/Z_i$ and the output voltage V_{out} will be $V_{out} = A_d V_{diff}$ where A_d is the differential amplification factor of the amplifier.

This indicates that any difference ΔZ between the electrode–skin impedances will result in an unwanted differential voltage, due to V_{cm}, at the amplifier's input. This voltage is amplified A_d times at the amplifier output, regardless of the CMRR of the amplifier, and results in a power line interference added to the physiological signal. The amount of PLI is inversely proportional to Z_i and this is the main reason for having a large Z_i value. Since the most important common mode interference source is due to the power line, the value of Z_i at 50 Hz (or 60 Hz) must be provided by the manufacturer. Alternatively, R_i and C_i may be provided and Z_i can be computed with eq (1).

Let us consider Fig. 2d or Fig. 11 and an amplifier whose input impedance is due to a capacitor $C_i = 10$ pF in parallel to a resistance $R_i > 1$ GΩ (Fig. 2d). Its input impedance at 50 Hz would be about 300 MΩ (mostly due to C_i). If $V_{cm} = 1V_{RMS}$ and $\Delta Z = Z_{e1} - Z_{e2} = 0.1$ MΩ (Piervirgili, Petracca and Merletti, 2014), we would have a ratio $\Delta Z/Z_i = 0.33 \cdot 10^{-3}$, generating a differential input signal of 0.33 mV$_{RMS}$ for each Volt of V_{cm}. This value is quite comparable with the sEMG signal magnitude and is proportionally larger for larger V_{cm} values (values of V_{cm} near 5 V are not uncommon). Eq. (2) (Section 5.1) can now be rewritten as:

$$V_{out} = V_{cm}A_{cm} + V_{cm}A_d\Delta Z/Zi + A_d V_{EMG} \tag{3}$$

where the third term of the right member of the equation is the one of interest and the first two terms should be minimized. If both sides of Eq. (3) are divided by A_d we obtain V_{in-eq}, representing the equivalent input voltage obtained from V_{out}. That is:

$$V_{in-eq} = V_{out}/A_d = V_{cm}(A_{cm}/A_d + \Delta Z/Zi) + V_{EMG} \tag{4}$$

From Eq. (4) we see that $A_{cm}/A_d = 1/CMRR$ should be small and therefore CMRR should be large.

We also see that $\Delta Z/Zi$ and $1/CMRR$ have the same importance and therefore an expensive amplifier with extremely high CMRR is not justified unless we are able to match Z_{e1} and Z_{e2} very well by proper skin treatment. This is the reason for having small and similar electrode–skin impedances (Fig. 3c). Some sEMG equipment has an impedance tester indicating some estimate of Z_{e1} and Z_{e2} but the frequency of measurement is often not indicated by the manufacturer.

It is obvious that it is desirable to reduce V_{cm} as much as possible. One improper way to reduce V_{cm} is to connect the subject to ground as was done by some old-time ECG technicians. This procedure is unsafe since it provides a current path, through the subject, to ground allowing 50 Hz currents due to faulty equipment, connected to the power line, to flow into the subject's body. Some proper ways to reduce V_{cm} at the input of the electrodes-amplifier system are a) lowering the reference electrode impedance by increasing its surface or b) using system floating (i.e. low C_p values in Fig. 11) with respect to ground. Several techniques are available to reduce the reference electrode impedance (Winter and Webster, 1983b; Webster, 1984) while it is possible to lower C_p designing a battery powered, floating and miniaturized system.

In summary, the main factors determining the PLI are: 1) the common mode voltage at the input of the electrode-amplifier system, 2) the value of CMRR of the front-end amplifier, 3) the value of the input impedance of the front-end amplifier at 50 Hz (or 60 Hz), 4) the value of the electrode–skin impedance unbalance (ΔZ), that must be minimized by proper skin treatment.

6.1.2. "Driven Right Leg" (DRL) circuit

The PLI can be reduced by reducing V_{cm}. Choosing an amplifier with a high common mode rejection ratio (CMRR) would affect only the first of the two terms on the right-hand side of Eq. (3) and Eq. (4). V_{cm} appears in both terms and can be reduced (up to a point) e.g. by reducing the parasitic coupling C_1 with the power line, that is by keeping power cables and equipment at some distance from the subject and the amplifier. However, this solution is sometime physically impossible to achieve or not sufficient. The same problem exists in electrocardiography where V_{cm} is often reduced by a technique called "Driven Right Leg (DRL)" which consists in taking (from the internal circuitry of the front-end amplifier or from the subject himself) the V_{cm} present on the subject and reapplying it to the subject's right leg (hence the name)
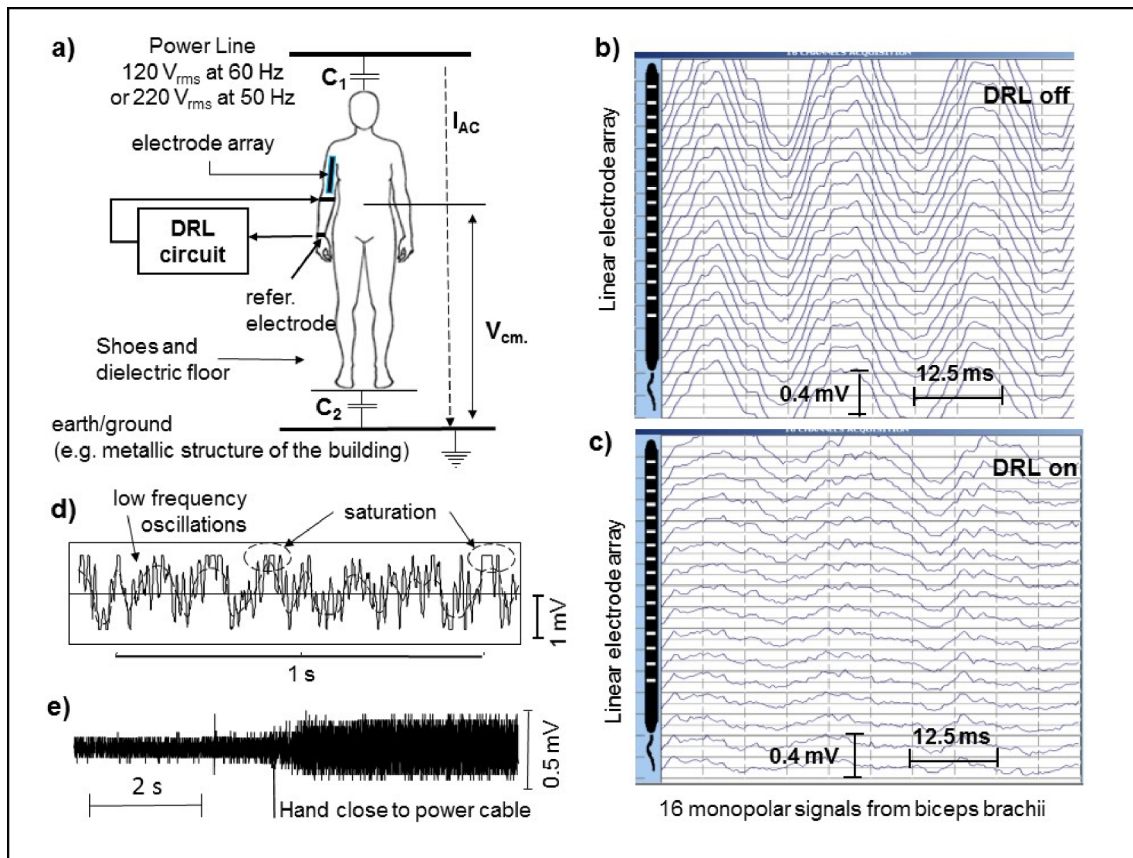
Fig. 12. Examples of power line interference (PLI). a) the parasitic capacitances C_1 and C_2 form a path between the power line and the earth/ground, generating a common mode voltage V_{cm} of the order of up to few V and a current I_{AC} of the order of tens of nA. Both can be reduced by reducing C_1, that is by keeping the subject away from power cables and equipment. The Driven Right Leg (DRL) circuit provides partial cancellation of V_{cm} by feeding back V_{cm} with opposite phase, as indicated in b) and c). b) example of PLI on the monopolar voltages detected by a linear electrode array, c) same as in b) with the DRL circuit active. d) example of recording affected by low frequency fluctuations and PLI large enough to cause saturation of the front-end amplifier and occasional clipping of its output voltage. e) example of increase of PLI when a hand of the subject is moved close to a power line cable, increasing C_1. (Courtesy of A. Gallina, C. Ritzel, and T. Vieira).

in opposite phase to reduce it. The DRL circuit in Fig. 12 performs this task. Some sEMG equipment provides this option. Of course, cancellation of V_{cm} cannot be totally achieved but attenuations of 5–10 times are possible. Fig. 12b and c show 16 monopolar channels obtained from a linear array of 16 electrodes applied on a relaxed biceps brachii without and with DRL.

Fig. 12d shows one sEMG channel affected by large slow fluctuations and 50 Hz interference causing occasional "saturation", that is, clipping of the signal at the amplifier's supply voltages V_s^+ and/or V_s^- (Fig. 2d). The signals depicted in Fig. 12d and e are "referred to the input", (or are "the equivalent input signal"); that is, they are obtained by dividing the output signal by A_d in order to allow comparisons with the sEMG signal detected by the electrodes. The signal in Fig. 12e shows the effect of moving a hand close to a power cable (220 V, 50 Hz). If the power line interference cannot be removed from the sEMG signal using the DRL and other techniques indicated above, other options can be considered, as described in the following subsections.

6.2. Reduction of power line interference by post processing

This section may or may not be considered as related to sEMG pre-processing because it describes operations performed after the A/D conversion. However, reduction of PLI by digital processing is a form of pre-processing that may be required before any further processing is performed on the digitized sEMG signal. It is important to underline that it is highly preferable to reduce the level of PLI at the source, avoiding digital manipulation of the collected sEMG signal. Therefore,

the user should be familiar with the problems and possible solutions described in Section 6.1.

6.2.1. Digital notch filters

A way to eliminate the power line interference from the sEMG signal is to filter the signal with a narrow band-reject filter centered at 50 Hz or 60 Hz. This procedure introduces a "notch" in the amplitude and power spectra of the signal and is called a "notch filter", as indicated in Fig. 9. Digital notch filters can be applied to the digitized signal (after the A/D conversion). They are sharper and more stable but also modify the shape of the signal because of their effect on the phase of the signal harmonics outside the rejected band.

Very often the PLI includes harmonics of the fundamental frequency (at 100 Hz, 150 Hz, 200 Hz, etc. or at 120 Hz, 180 Hz, 240 Hz, etc.). Consequently, the interference is no longer sinusoidal, although it may be recognized by its characteristic period of 20 ms (or 16.6 ms at 60 Hz). Multiple notch filters may be applied, thus resulting in further alteration of the original signal. This solution is not recommended and the alternative solution of "spectral interpolation" may be considered.

6.2.2. Spectral interpolation

Fig. 13a shows the amplitude spectrum (magnitude of the Fourier transform computed, in this case, over a 20 s recording) of a monopolar sEMG signal collected from back muscles (erector spinae). Spectral lines at 50 Hz, 100 Hz, 200 Hz, and other even harmonics are evident in this case, but both odd and even (or mostly odd) harmonics are present in other cases. The spectral interpolation technique, proposed by Mewett
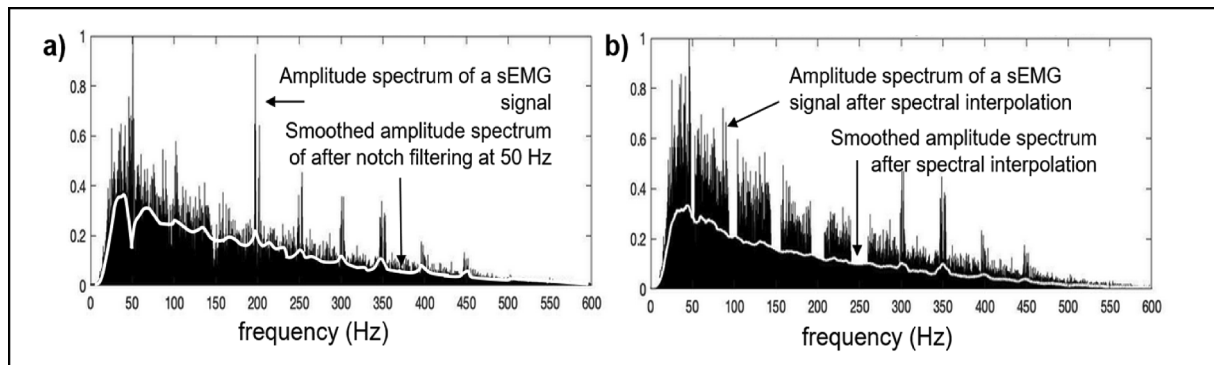
Fig. 13. Spectral interpolation. Example of amplitude spectrum (magnitude of the Fourier transform) of a 20 s long sEMG recording. Spectral lines (harmonics) of the signal are $1/20 = 0.05$ Hz apart. Large spectral lines are present at 50 Hz and at its even harmonics (more often they are present at the odd harmonics or at both). a) local effect of a notch filter at 50 Hz, b) amplitude spectrum after removal and linear interpolation of a bandwidth of $\pm$ 2 Hz around 50 Hz, $\pm$ 4 Hz around 100 Hz, $\pm$ 6 Hz around 150 Hz, $\pm$ 8 Hz around 200 Hz and $\pm$ 10 Hz around 250 Hz. Inverse Fourier transform of the interpolated amplitude and phase spectra provides a "clean" signal with no PLI and acceptably small modifications. The white lines depict the smoothed spectrum after notch filtering (a) or interpolation (b).

et al. (Mewett, Reynolds and Nazeran, 2004), consists in removing the spectral lines in the neighbourhood of the line frequency (and its harmonics) from the amplitude spectrum of the signal. These lines are then replaced with new ones obtained by interpolating a group of spectral lines preceding and following the removed ones. European power stations usually maintain the line frequency within 49.5 Hz to 50.75 Hz but this range might be expanded to 47.5 Hz to 51.5 Hz (European Network of Transmission System Operators for Electricity, 2014) in particular conditions. Fig. 13b show the spectrum depicted in Fig. 13a after the spectral interpolation process has been applied to the first five harmonics of the power line frequency. Other spectral lines are not modified by this operation. The inverse Fourier transform of the modified spectrum is then computed to obtain a good approximation of the interference-free input signal. This is a relatively simple off-line digital method to remove PLI. If the algorithm is applied to a signal free from power line interference, the modification of the signal is minimal and acceptable in view of further processing. Of course, it is not so in the case of a notch filter.

6.2.3. Other methods to reduce the power line interference

In some cases, the exact frequency and phase of the PLI can be obtained or can be estimated from the signal itself. The interference waveform can then be adaptively identified and subtracted from the original signal (Glover, 1977; Keshtkaran and Yang, 2014). This technique is often used in EEG, where the problem is even more serious than in ECG or EMG, given the lower signal amplitude.

In electrocardiography, the ECG derivations use the "Wilson node" as a virtual voltage reference. The Wilson node (W) reference voltage V_W is the average of the left arm (LA), right arm (RA) and left leg (LL) potentials and therefore is a reference whose PLI is the average of the three interferences, that is V_{cm}. The three leads $V_{LA} - V_W = V_L$, $V_{RA} - V_W = V_R$ and $V_{LL} - V_W = V_F$ have a strongly reduced residual PLI due to the differential operation. The same concept can be applied to sEMG detected from an electrode array, by creating a "filtered virtual reference" (Botter and Vieira, 2015).

7. Sampling and A/D conversion

Electrophysiological signals, such as sEMG, are analog signals. An analog signal is defined as a physical variable assuming a specific amplitude value for each time instant. In order to be stored and processed by computers they must be sampled, and each sample must be converted in digital form, that is into a binary number. In this way, it is possible to associate a number to each sample value. Binary numbers use only two ciphers: 0 (low state) and 1 (high state) instead of 10 (0 to

9) in the decimal notation. Numbers represented using a binary representation contain a sequence of these ciphers (0 s and 1 s), named bits.

The decimal representation of a natural number containing N ciphers, can describe values between 0 and $(10^N - 1)$ (e.g. a number with 4 ciphers can contain all numbers between 0000 and 9999), a number containing N bits can assume all values between 0 and $(2^N - 1)$. Given a number represented in binary form, the right-most bit is named Least Significant Bit (LSB) while the left-most bit represents the Most Significant Bit (MSB). The conversion of sEMG values into binary numbers is usually done by means of a digital device such as a Personal Computer or a Mobile Device (Smartphone or Tablet) (Webster, 2013).

7.1. Basic concepts and definitions related to the A/D conversion

The conversion of a signal in binary numbers is done by means of the Analog-to-Digital Converter (ADC or A/D converter). The A/D of Fig. 14 outputs a digital signal, coded in binary form, whose value is proportional to the analog voltage signal present at its input. Successively, the digital signal can be acquired by a digital device though a wired (e.g. USB) or wireless (e.g. Wi-Fi) digital peripheral. The features characterizing an A/D converter are: 1) the resolution, expressed in number of bits (N); 2) the input range (V_{FS}), expressed in Volts (V) and 3) the conversion time (t_c, μs).

The A/D resolution is defined by the number of bits (N) of the A/D converter. Consequently, an A/D converter having N bit resolution will convert analog signals into numbers between 0 and $(2^N - 1)$.

For the 8-bit case of Fig. 14 the range is between 00000000 to 11111111, that is 256 values. The full-scale input range of an A/D converter (V_{FS}) represents the signal voltage range that can be converted into numbers (digitized). Consequently, the smallest amplitude variation of the analog input signal that can be converted into two different numbers is $V_{LSB} = V_{FS} / (2^N - 1)$.

The conversion time is the time needed by an A/D converter to convert an input analog signal into a number. In order to guarantee a successful conversion, it is fundamental that the input signal will not vary of more than V_{LSB} within this time interval.

It is therefore important to guarantee that: 1) the signal will not vary during the conversion interval (hold function); 2) the signal will be sampled at regular time intervals (sample function). To this end, a special circuit, named "sample & hold" (S/H), is inserted between the signal conditioning chain and the A/D converter (Fig. 14). The A/D conversion of the sEMG signal requires values of t_c and N that are easy to achieve with the current technology.

7.2. Sampling

The sampling process implies the transformation of the input signal from the analog, continuous domain to a sequence of samples, as depicted in Fig. 15 This operation results in a loss of information due to the fact that, a) after sampling, we no longer know how the signal is in between samples and b) a sample cannot be stored with its exact value but can only take the values allowed by the A/D converter (see Table 1). It can be shown, and it is intuitive, that if the sampling frequency is "sufficiently high", the sEMG signal can be stored without loss of information and can therefore be "reconstructed" exactly, as discussed in the following.

With reference to Fig. 15a and b, two phenomena related to the signal sampling are evident:

(1) the converted signal is an approximation of the input signal due to the finite resolution of the A/D converter (i.e. finite number of values) and the finite sampling frequency (i.e. finite number of samples per second);
(2) by increasing the sampling frequency, it is possible to better represent fast variations of the signal and thus to better reconstruct the analog signal from its digital form.

Given a signal whose highest frequency component (harmonic) is B Hz, the Shannon-Nyquist criterion, referred to as "sampling theorem", defines the minimum sampling frequency (f_s) required to avoid loss of information due to the sampling process as $f_s > 2B$. If the Shannon-Nyquist criterion is satisfied it is possible to exactly reconstruct the original analog signal from the digital one. If the Shannon-Nyquist criterion is not satisfied and $f_s \leq 2B$, the information contained in the digital signal will not be the same contained in the analog one, resulting in the so called "aliasing effect" (Blinowska and Zygierewicz, 2011).

Fig. 15a and b show the effect of the improper sampling process on the input signal. It is evident that the higher is the sampling frequency (above 2B samples/s), the better is the representation of the analog signal in a binary form. The bandwidth of the sEMG extends to 450–500 Hz and commonly used sampling frequencies are near or above 2000 samples/s. The sampling frequency of 2048 samples/s if often used because it offers some technical advantages.

7.2.1. Spatio-temporal sampling.

The above considerations apply for sampling an image in space. A sEMG image (evolving in time) can be obtained by placing a grid of equally spaced electrodes, taking samples on the skin. Each time-varying signal corresponds to a pixel of this image. The sampling frequency in space is expressed in samples/meter (samples/m) and should be greater than 100–200 samples/m which means an inter-electrode distance (IED) of less than 10–5 mm. IED = 10 mm, corresponding to a
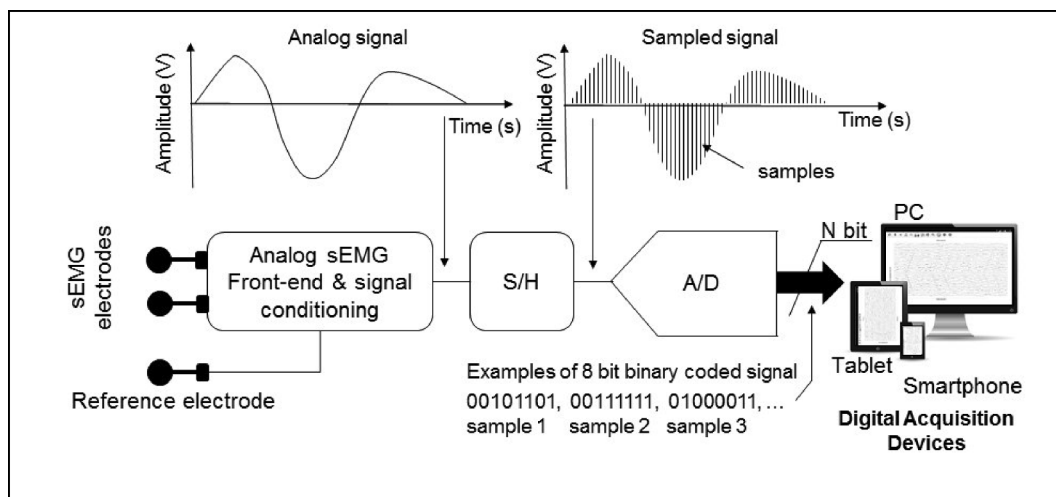

Fig. 14. sEMG acquisition chain. Signals are detected by means of surface electrodes placed on the skin. The signal is amplified, conditioned, sampled (S/H), digitally converted (A/D), and transferred to a digital device through a communication interface (e.g. USB, Wi-Fi, etc.).
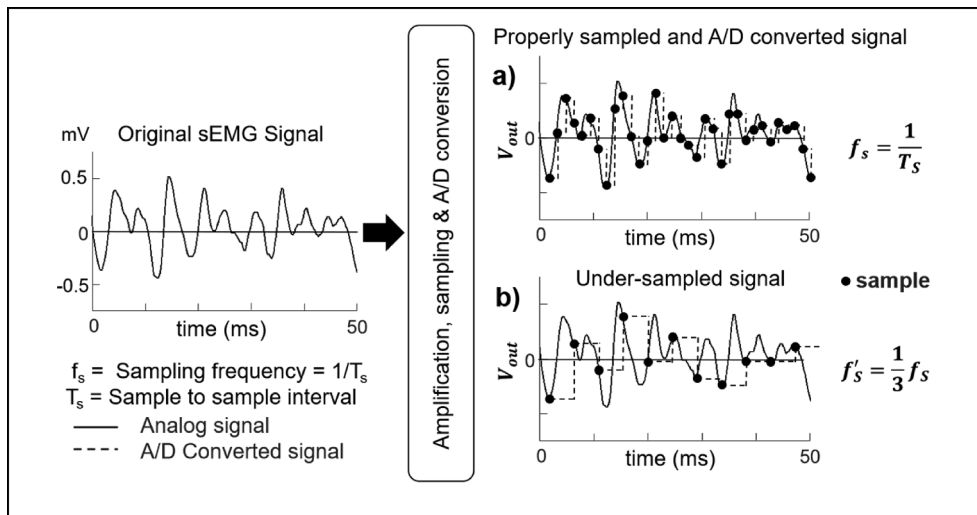

Fig. 15. Sampling and A/D conversion. A sEMG is sampled (black dots) and quantized (converted) into a digital signal (dashed line) respectively through a Sample&Hold and an A/D converter. a) The signal is sampled at a given frequency f_s (for clarity one sample every 5 is shown). b) The same signal is under-sampled at one third of the previous sampling frequency. It is possible to observe that the digitally converted signal results more distorted than the previous one. For clarity of representation, the sampling frequency in the figure (approximately 125 Hz) does not meet the Shannon-Nyquist criterion.

Table 1
Relation between number of bits of the A/D converter, number of levels, V_{LSB} and input referred resolution (voltage difference corresponding to the least significant bit). The amount of Data Memory required for 1 s long recording for a single EMG channel sampled at fs = 2048 Hz in Bytes is related to the resolution of the A/D converter. The numbers in parentheses indicate the effective amount of memory required if compression algorithms are not used. Compression algorithms eliminate leading zeros in a byte and reduce memory requirements.

Number of bits N of the A/D converter	Number of Levels: 2^N (0 to 2^N-1)	V_{LSB} ($V_{FS} = \pm 5$ V) $V_{LSB} = 10/(2^N - 1)$	Input referred resolution for amplifier A = 1000 and $V_{FS} = \pm 5$ V	Data Memory required for 1 s long recording for a single sEMG channel sampled at $f_s = 2048$ Hz (Bytes)
8	256	39.06 mV	39.06 μV	2048
10	1024	9.77 mV	9.765 μV	2560 (4096)
12	4096	2.441 mV	2.441 μV	3072 (4096)
14	16,384	0.610 mV	0.610 μV	3584 (4096)
16	65,536	0.152 mV	0.152 μV	4096
24	16,777,216	0.0006 mV	0.0006 μV	6144

sampling frequency of 100 samples/m, introduces errors that are acceptable for most applications. Larger IEDs are acceptable for biofeedback and sEMG decomposition but not for image interpolation, estimation of image centroid or regions of activity or other forms of image processing. This issue has been discussed in a previous tutorial (Merletti and Muceli, 2019).

7.3. Quality of converted signals: Influence of the A/D resolution, errors and noise

The quality of the digitally converted signal is affected by the A/D converter resolution. Fig. 16a and b show the effect of a low A/D resolution for a sinusoidal signal sampled at a given sampling frequency. For a given amplitude and number of samples, the input signal is better represented in the digital domain if it can be discretized into a large number of digital values. The lower is the signal amplitude that we wish to accurately represent, the higher is the required A/D converter resolution, that is the higher must be the number of levels and, therefore, the number of bits (lower V_{LSB}).

Table 1 indicates the input referred resolution (V_{LSB}/Amplification) for different A/D resolutions. Increasing the A/D resolution leads to larger file sizes and higher requirement in terms of data transmission and storage capacity of the acquisition device (e.g. the PC). Furthermore, a proper A/D resolution implies V_{LSB} to be much smaller than the peak-to peak noise generated by the electrode–skin interface. For example, if the noise has an approximate peak-to-peak amplitude of 5 μV to 10 μV, a resolution of 0.5 μV- 1.0 μV would be sufficient to properly sample and convert signal and noise, at the proper frequency. An A/D resolution with N = 12 bit could be sufficient to acquire good quality sEMG signals but, considering the nonlinearities of the A/D converter

(discussed below), this value is practically barely acceptable, and 14–16 bit should be preferred.

The quantization error (V_{eq}) is defined as the difference, for a given sample, between the input voltage V_{IN} and the voltage corresponding to the numerical value converted by the A/D (V_{AD}):

$$V_{eq} = V_{IN} - V_{AD} \tag{5}$$

As an example, Fig. 17 shows the trend of the quantization error for an ideal A/D converter when a ramp input signal is applied. The quantization error varies between 0 and V_{LSB} and is a function of 1) the input signal type (sine, ramp, etc.) and, 2) the A/D converter resolution. The quantization error introduced by the A/D converter can be considered as an additive noise to the input signal.

A/D converters are affected by other sources of errors which introduce noise (Texas Instruments, 1995). The noise introduced by the A/D conversion process is described by the signal to noise ratio due to the quantization error (SNR_q) as the ratio between the power of the input signal and the power of the quantization noise. The higher is SNR_q the lower is the quantization noise introduced by the A/D conversion and consequently the higher is the quality of the converted signal. For example, an A/D converter of 12 bit can effectively convert up to 10 bit without errors. In this case, considering an input signal of 1 mV_{RMS} and $V_{FS} = \pm 5$ V, the input-referred noise added by the A/D sampling process (V_{eq}/A_d) is about 2 uV_{RMS}, that is comparable to that introduced by the electronics and the electrode–skin interface. In these circumstances, 12 bit A/D converters are barely acceptable. In fact, an A/D converter does not have an ideal behavior because other errors can lower the effective resolution of the A/D converter. A/D converted manufacturers usually express the contribution of these errors to the A/D conversion noise through the so-called Quantization and Distortion
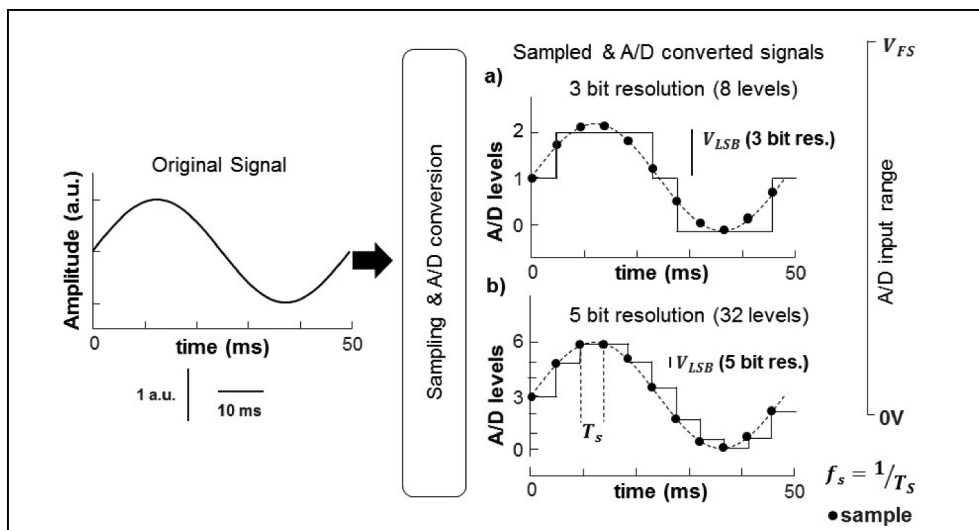
Fig. 16. Effect of the A/D resolution on a digitally converted signal for a fixed sampling frequency. A sinewave is sampled (black dots) and converted (continuous black lines) into a digital signal using 3-bit (a) or 5-bit (b) resolution of the A/D converter. In the first case it is possible to observe that the Least Significant Bit (LSB) has a wider (four times) amplitude (V_{LSB}) of that obtained using 5-bit resolution. It is evident that the signal is better approximated in b) than in a). a.u. = arbitrary unit.
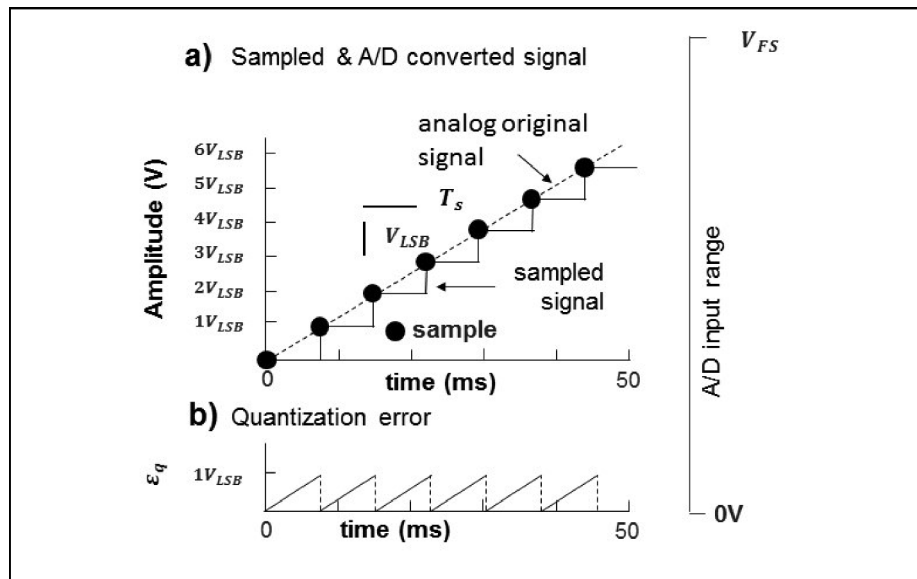
Fig. 17. a) Quantization error. A ramp signal is sampled (black dots) and converted (continuous black line) into a digital signal. b) The quantization error (ε_q), varies between 0 V (right after the conversion has occurred) and V_{LSB} (immediately before the new sample is acquired).

SNR (SNDR).

Given a certain SNDR declared for a given A/D converter, it is possible to calculate, the Effective Number Of Bits (ENOB) that can be considered clean from the A/D conversion noise. As an example, an A/D converter with N = 16-bit resolution and SNDR = 86 dB behaves like an ideal A/D converter with ENOB = 14 bit. Therefore, it is important that a device manufacturer would declare also the Effective Number of Bits of the A/D converter and not only the corresponding A/D resolution that does not take into account A/D quantization errors and non-linearities.

8. Recommendations for best practices

The user operating inside the European Union shall check that the Medical Device is CE marked in accordance the EU Directives (CEE 93/42 (until May 2021), 2007/47/CE (until May 2021), and MDR 217/745/CE) regulating the Medical Devices fabrication and commercialization. Other Directives apply for USA (FDA Directives), Japan or China users. The compliance of sEMG devices with the above-mentioned Directives is mandatory.

The compliance of the device with at least the following International Standards is also desirable:

- IEC 60601-1: Medical electrical equipment – Part 1: General requirements for basic safety and essential performance. (https://webstore.iec.ch/publication/2612)
- IEC 60601-2-40: Part 2-40: Medical electrical equipment – Particular requirements for the basic safety and essential performance of electromyographs and evoked response equipment. (https://webstore.iec.ch/publication/25681)

The proper instructions for use (IFU) and guidelines must be provided with the sEMG acquisition system and the device should result free from unacceptable hazards due to system faults, improper use or, whenever possible, misinterpretation of results that may depend on the user's insufficient competence.

The main purpose of this tutorial is to make the current and future users of sEMG aware of the issues, problems, technical equipment specifications, and possible errors and responsibilities, associated to the detection and conditioning of this signal. A background knowledge is necessary to assess the quality of the signals, interpret and process

them, communicate results, make clinical decisions, allow other operators to repeat the measurements. For these reasons, sEMG detection and conditioning modalities must be described in reports, thesis, manuals, publications and any other form of dissemination and sharing of experience and knowledge, to allow other investigators or clinicians to understand the adopted procedures and repeat tests and measurements in the same conditions, thus ensuring the repeatability of the experiments and a proper transfer of knowledge.

All features of the sEMG signal are affected by the quality of the signal, and consequently by the detection modalities and by the contaminations discussed in the previous Sections, largely dependent on the user's care and competence. This problem concerns all bioelectric signals and has been addressed for ECG and EEG (Radüntz, 2018; Zhao and Zhang, 2018) as well as for sEMG (Sinderby, Lindström and Grassino, 1995; McCool et al., 2014). The quality of the signal can, to a limited degree, be tested automatically. For example, PLI or amplifier saturation can be automatically detected and activate a warning system based on artificial intelligence and classification procedures of bioelectric signals (to help the user in deciding if a signal is of acceptable quality or not (McCool et al., 2014; Zhao and Zhang, 2018). Although this approach can point out gross anomalies, it can neither replace the intelligent expert human observation of the original signal nor correct errors in the acquisition and conditioning process. This approach for automatic detection and warning about "bad channels" showing large artifacts or interference may be necessary when electrode arrays are used, and human visual check of many channels would be very time consuming.

Some of these issues have been investigated and recommendations have been provided 20 years ago (Hermens et al., 2000) (www.seniam.org) as well as more recently (Besomi et al., 2019; Merletti and Muceli, 2019). However, researchers or clinicians may need or choose not to follow these recommendations and explain the reason for not doing so in their reports or publications.

8.1. Recommendations concerning electrodes and detection modalities

Detection modalities deal with the choice and description of the electrode system and the skin treatment. The features of the detection system, the skin treatment, the electrode montage (monopolar, single differential, other spatial filters), dramatically affect the signal quality, the quality of information, the level of PLI, etc. The following

information must be reported in order to allow reproduction of the work:

1. Material (e.g. Ag, AgCl, Au, etc), size and shape (bar, circular) and dimensions (length, diameter), manufacturer of the electrodes;
2. Use of gel (gel type, manufacturer);
3. Monopolar, single differential or other spatial filters or geometrical arrangements used;
4. Skin treatment (rubbing with alcohol is not recommended, type and manufacturer of abrasive gel should be reported) (Cattarello and Merletti, 2016);
5. Interelectrode distance and electrode location with respect to the fiber direction, the innervation zone of the muscle, or anatomical references.
6. Fixation modalities and length of the electrode-amplifier connections. Possible use of shielded cables or power line reduction techniques.

Some of these issues have been discussed in a previous tutorial (Merletti and Muceli, 2019).

8.2. Recommendations concerning the front-end amplifier.

As mentioned in Section 5, some features of the front-end amplifier have a considerable impact on sEMG signal quality. They posit a set of criteria for purchasing a sEMG system.

Input impedance. High input impedance (at 50 Hz or 60 Hz) is desirable to reduce the PLI (see Eq. (3) and (4)). The input impedance of the front-end amplifier should be adequate to the type of system.

It should be at least 300 MΩ at 50 Hz or 60 Hz if small electrodes (e.g. 3 mm diameter) and non-floating amplifiers are used, and at least 80 MΩ if small electrodes and battery-powered amplifiers are used (in this case the common mode voltage due to PLI is lower). As indicated above, some manufacturers erroneously provide only the input resistance.

Common mode rejection ratio (CMRR). The CMRR should be at least 90 dB in order to ensure proper rejection of common mode signals at the input of the front-end amplifier.

Setup. Power cables connected to the sEMG equipment, to the computer or to nearby equipment should not be near the subject or the operator to reduce parasitic coupling between the amplifier, or the subject, with the power line (Fig. 12) and consequently the common mode voltage.

Amplification factor (gain). Some sEMG amplifiers have adjustable amplification values (e.g. 100, 1000, 2000) but most have a fixed amplification lower than 1000. Consider that a low amplification, associated with an improper A/D converter full scale, implies a small signal at the input of the A/D converter and therefore the involvement of a limited number of levels (Section 7.3 Table 1 and Fig. 17). The problem is less relevant if the A/D converter has 16 bits (65536 levels) since a sufficient number of levels is available even for a small signal (Section 7.3). On the other hand, a large gain (or a large signal) results in an amplifier output possibly reaching the limits of the supply voltages and causing saturation (Fig. 5). As an example, an acquisition system having 16-bit A/D resolution, 3.3 V A/D full scale range and amplification equal to 200 V/V may be considered a good choice to acquire sEMG signals. Expensive A/D converter with high resolution (e.g. 24 bit) are justified only in case of extremely low amplification

Table 2
Checklist for preparing and reviewing reports and manuscripts dealing with sEMG.

Topic	Item	Description of item	Considerations and main references
Medical Device Regulation Compliance	1	Is the Electromyograph CE or FDA marked?	Medical device must be CE (for European users) or FDA (United States) marked in order to be used and ensure proper performance and safety.
	2	Is the the Electromyograph complying with International Standards?	It is desirable that the device is compliant with international standard to guarantee its essential performance and safety.
Electrodes	1	Are electrode material, size, shape, inter-electrode distance, and manufacturer reported?	sEMG features are affected by electrode size and interelectrode distance (Merletti and Muceli, 2019)
	2	Is the skin treatment described? If gel is used, is the manufacturer reported?	Power line interference, noise, and artifacts are affected by skin treatment (Piervirgili, Petracca and Merletti, 2014)
	3	Is the electrode position with respect to the muscle's innervation zone or with respect to anatomical landmarks reported? Is the orientation with respect to fiber direction mentioned?	The amplitude of sEMG detected in SD modality is smaller when electrodes are on or near the innervation zone or not aligned with the fiber direction.
	4	Is a spatial filter used? Is it described?	sEMG is different depending on the monopolar, SD or DD detection modality.
	5	Are modalities of electrode and cable fixations reported?	Poor electrode or cable fixation to the skin may cause large movement artifacts.
Amplifier	1	Is the input impedance of the amplifier reported at the power line frequency? Or are input resistance and capacitance reported?	The amplifier input impedance (at 50 Hz or 60 Hz) is one of the factors determining PLI.
	2	Is the CMRR of the amplifier reported at the power line frequency?	The CMRR (at 50 Hz or 60 Hz) is one of the factors determining PLI.
	3	Is the RTI noise introduced by the amplifier low enough?	The RTI amplifier noise level should be less than $2\mu V_{RMS}$.
	4	Is the gain of the amplifier properly set to avoid saturation when the sEMG is large?	Amplifier saturation must be avoided because the distortion cannot be corrected.
Filters	1	How is PLI reduced? Is DRLused? Are the filter properties (cut off frequency, type and order of each filter) reported?	The cut-off frequency of the high- pass filter should be ≤ 20 Hz (De Luca et al., 2010; Merletti, 2010). The cut-off frequency of the low-pass filter is less critical.
	2	Is a notch filter used to reduce power line interference? Are the filter type and order and the rejected bandwidth reported? Is spectral interpolation (or other techniques) used to limit PLI?	A notch filter attenuates the power line interference but also alters the sEMG amplitude and spectral features. Spectral interpolation may be preferable (Section 6).
A/D Conversion	1	Are the A/D converter features (number of bits, voltage range, SNDR, ENOB) declared?	The A/D converter features affect the signal quality in terms of input-referred resolution and quantization noise
sEMG signal quality testing	1	Has the sEMG signal been visually checked for lack of PLI and for lack of saturation at high sEMG amplitudes?	Amplifier saturation must be avoided because the signal distortion cannot be corrected.
	2	Has the background noise level been visually checked when the muscle of interest is relaxed?	Electrode-skin and amplifier noise should be less than 5 μV_{RMS} (15–20 μV_{pp}).
	3	Have the electrode contact stability and cable fixation been checked by slightly tapping on the skin near the electrodes?	Large artifacts due to slight tapping on the skin indicate poor electrode stability.

(e.g. less than 10 V/V).

Input referred noise. A good bioelectric signal amplifier has 1–2 μV_{RMS} referred-to-input voltage noise (RTI) in the bandwidth 20–500 Hz. This is acceptable in view of the fact that the electrode–skin junction and the A/D converter introduce a larger noise. Because of this reason, expensive low-noise (below 1 μV_{RMS}) front-end amplifiers are not warranted.

8.3. Recommendations concerning signal filtering in the time domain.

The manufacturer should indicate the main features (filter type, order, corner frequencies) of the analog conditioning circuitry used.

High pass filtering. The low frequency portion of the sEMG spectrum (1–30 Hz) is affected by fluctuations of the half-cell potentials (V_b in Fig. 2), by the slow tail of the repolarization phase of muscle fiber action potentials, by the discharge frequencies of the motor units (about 6–30 Hz) and by artifacts (De Luca et al., 2010). The cut-off frequency of the high pass filter is therefore a compromise that depends on the purpose of the sEMG measurement. Corner frequencies of high pass filters are reported in the literature in the range from 5 Hz to 30 Hz with the most common range of 10–20 Hz. Filters of order ≥ 2 are recommended.

Low pass filtering. The sEMG power spectrum is skewed and shows a long tail (Fig. 8 and Fig. 13) merging with the background noise level at about 350 Hz-450 Hz. Since a small portion of the sEMG power is accounted for by the frequency components > 350 Hz the low pass cut-off frequency is usually in the range 400–500 Hz and is not critical. Analog filters of order ≥ 2 are commonly used. The cut-off frequency of the analog low pass filter must be less than half the sampling frequency

Notch filtering. Some sEMG system include the option for analog or digital notch filtering of the PLI. This modifies the spectral features of the sEMG and is not recommended if such features are of interest. In any case, the manufacturer should indicate the width of the rejected band and the notch filter order and type (analog or digital).

8.4. Recommendations concerning sampling in time and A/D conversion.

Sampling. To avoid aliasing, the sampling frequency must be greater than twice the highest frequency of interest of the sEMG. Sampling frequency is usually > 1500 Hz but 2000 Hz or 2048 Hz are preferred values.

A/D conversion. The sampled sEMG values are converted into binary numbers that can take any of 2^N values (from 0 to $2^N - 1$) where N is the number of bits of the A/D converter. Recommended number of bits is ≥ 12 but 16 is preferred because it provides acceptable quantization errors even for small signals amplified with a fixed gain. A resolution (difference between adjacent levels) of ≤ 0.5 μV is recommended. The manufacturer should declare the SNDR, the Effective Number of Bits (ENOB) of the A/D converter and the corresponding input-referred signal resolution of the acquisition device.

8.5. Recommendations concerning sampling in space.

A grid of electrodes samples the sEMG signal in space and provides an image for each sample in time. In order to extract the spatial information contained in the image and to allow interpolation of the image, the sampling frequency in space should be > 200 samples/m (that is the interelectrode distance (IED) should be < 5 mm) but this value implies an high number of channels to cover the entire surface of large muscles (Merletti and Muceli, 2019) and a large amount of data. Compromise values are IED = 8 mm or 10 mm if some aliasing can be tolerated. This is a requirement only for applications that involve image manipulations or interpolation. Since spatio-temporal filtering is

applied also to the classical bipolar detection, the user should be aware of it when IED > 10 mm.

8.6. Other general recommendations

It is a good practice to visually check the original sEMG signal before processing it. Once amplitude, spectral, or other features are computed, correction for PLI, noise or artifact contamination is impossible. Surface EMG acquisition systems that allow visualization of the signal are therefore preferable to systems that only provide results of processing (such as RMS amplitude). If such option is not available, at least verification that the sEMG amplitude is at an acceptably low (noise) level when the muscle of interest if fully relaxed is necessary. Table 2 provides a checklist of the information that should be provided by the user in a report or manuscript dealing with sEMG. Some of the information should be available from the manufacturer.

9. Concluding remarks

Proper detection, amplification and filtering are fundamental steps in sEMG acquisition and remarkably affect its processing and interpretation. While engineering problems, such as circuitry design and software development, are designer's tasks, the purchase, the proper use of equipment, and the proper reporting of results, are clinician's responsibilities. In addition, clinicians should interact with the engineering experts and express their demands, requirements and specifications that equipment should meet, thereby interacting with the phase of hardware and software design. This and other tutorials attempt to increase the level of technical competences required from clinical sEMG users that are going to be progressively introduced as an integral part of education, training programs and curricula of academic institutions and courses.

References

Barbero, M., Merletti, R., Rainoldi, A., 2012. Atlas of Muscle Innervation Zones: Understanding surface EMG and its applications. 1st ed., Springer-Verlag Italia, Milano, Italy. doi: 10.1007/978-88-470-2463-2.

Bareket, L., et al., 2016. Temporary-tattoo for long-term high fidelity biopotential recordings. Scientific Reports 10 (6), 1–8. https://doi.org/10.1038/srep25727.

Basmajian, J.V., De Luca, C.J., 1985. Muscles Alive: their functions revealed by electromyography. https://doi.org/10.1227/01.NEU.0000028086.48597.4F.

Bates, J.B., Chu, Y.T., 1992. Electrode-electrolyte interface impedance: Experiments and model. Annals of Biomedical Engineering 20, 349–362. https://doi.org/10.1007/BF02368536.

Besomi, M., et al., 2019. Consensus for experimental design in electromyography (CEDE) project: Electrode selection matrix. Journal of Electromyography and Kinesiology 48, 128–144. https://doi.org/10.1016/j.jelekin.2019.07.008.

Blinowska, K., Zygierewicz, J., 2011. Practical Biomedical Signal Analysis Using MATLAB. 1st ed., CRC Press. doi: 10.1201/b11148.

Botter, A., et al., 2019. Development and testing of acoustically-matched hydrogel-based electrodes for simultaneous EMG-ultrasound detection. Medical Engineering and Physics 64 (1), 74–79. https://doi.org/10.1016/j.medengphy.2018.12.002.

Botter, A., Vieira, T.M., 2015. Filtered virtual reference: A new method for the reduction of power line interference with minimal distortion of monopolar surface EMG. IEEE Transactions on Biomedical Engineering 62 (11), 2638–2647. https://doi.org/10.1109/TBME.2015.2438335.

Burbank, D.P., Webster, J.G., 1978. Reducing skin potential motion artefact by skin abrasion. Medical and Biological Engineering and Computing 16 (1), 31–38. https://doi.org/10.1007/BF02442929.

Campanini, I., et al., 2020. Surface Electromyography: barriers limiting widespread use of sEMG in clinical assessment and neurorehabilitation. Frontiers in Neurology/Neurorehabilitation. https://doi.org/10.1007/BF02442929. (submitted for publication).

Cattarello, P., Merletti, R., 2016. Characterization of dry and wet Electrode-Skin interfaces on different skin treatments for HDsEMG. In: in *2016 IEEE International Symposium on Medical Measurements and Applications, MeMeA 2016 - Proceedings*, pp. 1–6. https://doi.org/10.1109/MeMeA.2016.7533808.

Cerone, G.L., Botter, A., Gazzoni, M., 2019. A Modular, Smart, and Wearable System for High Density sEMG Detection. IEEE Transactions on Biomedical Engineering 66 (12), 3371–3380. https://doi.org/10.1109/TBME.2019.2904398.

Cerone, G.L., Gazzoni, M., 2018. A wireless, minaturized multi-channel sEMG acquisition system for use in dynamic tasks. In: in *2017 IEEE Biomedical Circuits and Systems Conference, BioCAS 2017 - Proceedings*, pp. 1–4. https://doi.org/10.1109/BIOCAS.2017.8325129.

DeLuca, C.J., 2006. 'Electromygraphy', in *Encyclopedia of*. Medical Devices and Instrumentation.

DeLuca, C.J., et al., 2010. Filtering the surface EMG signal: Movement artifact and baseline noise contamination. Journal of Biomechanics 43, 1573–1579. https://doi.org/10.1016/j.jbiomech.2010.01.027.

Dobrev, D., Daskalov, I., 2002. Two-electrode biopotential amplifier with current-driven inputs. Medical and Biological Engineering and Computing 40 (1), 122–127. https://doi.org/10.1007/BF02347705.

Dobrev, D., Neycheva, T., Mudrov, N., 2005. Simple two-electrode biosignal amplifier. Medical and Biological Engineering and Computing 43 (1), 725–730. https://doi.org/10.1007/BF02430949.

European Network of Transmission System Operators for Electricity, E.-E.A., 2014. ENTSO2014. Available at: www. entsoe.eu.

Farina, D., 2006. Surface Electromyography (EMG) Signal Processing. In: Wiley Encyclopedia of Biomedical Engineering. doi: 10.1002/9780471740360.ebs1378.

Farina, D., Jensen, W., Akay, M., 2013. Introduction to Neural Engineering for Motor Rehabilitation, Introduction to Neural Engineering for Motor Rehabilitation. IEEE Press and J. Wiley. doi: 10.1002/9781118628522.

Fernández, M., Pallás-Areny, R., 2000. Ag-AgCl electrode noise in high-resolution ECG measurements. Biomedical Instrumentation and Technology 34 (2), 125–130.

Floyd, W.F., Silver, P.H.S., 1950. Electromyographic study of patterns of activity of the anterior abdominal wall muscles in man. Journal of anatomy 84, 132–145.

Gazzoni, M., 2015. Low cost inkjet printing for the fast prototyping of surface EMG detection systems. In: in *2015 IEEE International Symposium on Medical Measurements and Applications, MeMeA 2015 - Proceedings*, pp. 79–83. https://doi.org/10.1109/MeMeA.2015.7145176.

Glover, J.R., 1977. Adaptive Noise Canceling Applied to Sinusoidal Interferences. In: IEEE Transactions on Acoustics, Speech, and Signal Processing, pp. 484–491. doi: 10.1109/TASSP.1977.1162997.

Godin, D.T., Parker, P.A., Scott, R.N., 1991. Noise characteristics of stainless-steel surface electrodes. Medical & Biological Engineering & Computing 29, 585–590. https://doi.org/10.1007/BF02446089.

Griss, P., et al., 2002. Characterization of micromachined spiked biopotential electrodes. IEEE Transactions on Biomedical Engineering 49 (6), 597–604. https://doi.org/10.1109/TBME.2002.1001974.

Hermens, H.J., et al., 2000. Development of recommendations for SEMG sensors and sensor placement procedures. Journal of Electromyography and Kinesiology 10 (2), 361–374. https://doi.org/10.1016/S1050-6411(00)00027-4.

Hewson, D.J., et al., 2003. Evolution in impedance at the electrode-skin interface of two types of surface EMG electrodes during long-term recordings. Journal of Electromyography and Kinesiology 13 (3), 273–279. https://doi.org/10.1016/S1050-6411(02)00097-4.

Huigen, E., Peper, A., Grimbergen, C.A., 2002. Investigation into the origin of the noise of surface electrodes. Medical and Biological Engineering and Computing 40 (1), 332–338. https://doi.org/10.1007/BF02344216.

Jahanmiri-Nezhad, F., et al., 2015. A practice of caution: spontaneous action potentials or artifactual spikes? Journal of NeuroEngineering and Rehabilitation 12 (1), 1–5. https://doi.org/10.1186/1743-0003-12-5.

Kamen, G., Gabriel, D.A., 2010. EMG signal processing. Human Kinetics Publisher, Essentials of electromyography.

Keshtkaran, M.R., Yang, Z., 2014. A fast, robust algorithm for power line interference cancellation in neural recording. Journal of Neural Engineering 11 (2), 1–14. https://doi.org/10.1088/1741-2560/11/2/026017.

Kim, M., et al., 2018. Wireless sEMG system with a microneedle-based high-density electrode array on a flexible substrate. Sensors (Switzerland) 30 (18), 1–12. https://doi.org/10.3390/s18010092.

Koch, K.P., Schuettler, M., Stieglitz, T., 2002. Considerations on noise of electrodes in combination with amplifiers for bioelectrical signal recording. Biomedizinische Technik. Biomedical engineering 47, 514–516. https://doi.org/10.1515/bmte.2002.47.s1b.514.

Lu, F., et al., 2018. Review of stratum corneum impedance measurement in non-invasive penetration application. Biosensors 8 (2), 1–20. https://doi.org/10.3390/bios8020031.

McCool, P., et al., 2014. Identification of contaminant type in surface electromyography (EMG) signals. IEEE Transactions on Neural Systems and Rehabilitation Engineering 22, 774–783. https://doi.org/10.1109/TNSRE.2014.2299573.

Merletti, R., et al., 2009. Technology and instrumentation for detection and conditioning of the surface electromyographic signal: State of the art. Clinical Biomechanics 24 (2), 122–134. https://doi.org/10.1016/j.clinbiomech.2008.08.006.

Merletti, R., et al., 2010. Advances in Surface EMG: Recent Progress in Clinical Research Applications. Critical Reviews in Biomedical Engineering 38 (4), 347–379. https://doi.org/10.1615/CritRevBiomedEng.v38.i4.20.

Merletti, R., 2010. The electrode-skin interface and optimal detection of bioelectric signals. Physiological Measurement 31 (10), 1–4. https://doi.org/10.1088/0967-3334/31/10/e01.

Merletti, R., 2020a. www.robertomerletti.it. Available at: https://www.robertomerletti.it.

Merletti, R., 2020b. www.robertomerletti.it. Available at: https://www.robertomerletti.it/en/emg/material/teaching/module4.

Merletti, R., Bonato, P., 2008. Electromyography (EMG), Surface. In: Wiley Encyclopedia of Biomedical Engineering. John Wiley & Sons, pp. 1–21. doi: 10.1002/9780471740360.ebs1156.

Merletti, R., Farina, D., 2016. Surface Electromyography: Physiology, Engineering and Applications. Edited by R. Merletti and D. Farina. IEEE Press and J. Wiley. doi: 10.1002/9781119082934.

Merletti, R., Farina, D., Holobar, A., 2018. Surface Electromyography (sEMG). In: Wiley Encyclopedia of Electrical and Electronics Engineering. doi: 10.1002/047134608x.w8371.

Merletti, R., Muceli, S., 2019. 'Tutorial. Surface EMG detection in space and time: Best practices', *Journal of Electromyography and Kinesiology* 49, 1–16. https://doi.org/10.1016/j.jelekin.2019.102363.

Merlo, A., Campanini, I., 2016. Applications in movement and gait analysis. In: Merletti, R., Farina, D. (Eds.), Surface Electromyography: Physiology, Engineering and Applications. IEEE Press and Wiley Interscience, p. 447. doi: 10.1002/9781119082934.ch16.

Mewett, D.T., Reynolds, K.J., Nazeran, H., 2004. Reducing power line interference in digitised electromyogram recordings by spectrum interpolation. Medical and Biological Engineering and Computing 42 (4), 524–531. https://doi.org/10.1007/BF02350994.

Mitchell, D., 2016. Surface Electromyography: Fundamentals, Computational Techniques and Clinical Applications, 1st edn. Nova Science Publisher.

Pani, D., et al., 2019. Validation of Polymer-Based Screen-Printed Textile Electrodes for Surface EMG Detection. IEEE Transactions on Neural Systems and Rehabilitation Engineering 27 (7), 1370–1377. https://doi.org/10.1109/TNSRE.2019.2916397.

Piervirgili, G., Petracca, F., Merletti, R., 2014. A new method to assess skin treatments for lowering the impedance and noise of individual gelled Ag-AgCl electrodes. Physiological Measurement 35 (10), 2101–2118. https://doi.org/10.1088/0967-3334/35/10/2101.

Puurtinen, M.M., et al., 2006. Measurement of noise and impedance of dry and wet textile electrodes, and textile electrodes with hydrogel. Annual International Conference of the IEEE Engineering in Medicine and Biology - Proceedings 6012–6015. https://doi.org/10.1109/IEMBS.2006.260155.

Radüntz, T., 2018. Signal quality evaluation of emerging EEG devices. Frontiers in Physiology 9 (98), 1–12. https://doi.org/10.3389/fphys.2018.00098.

Russo, A., Merletti, R., 2017. 'Spatially Correlated Noise Among Electrodes in HDsEMG', in *ISB2017*. Brisbane, Australia Available at: https://isbweb.org/images/conferences/isb-congresses/2017/ISB2017-Full-Abstract-Book.pdf.

Shustak, S., et al., 2019. Home monitoring of sleep with a temporary-tattoo EEG, EOG and EMG electrode array: A feasibility study. Journal of Neural Engineering 16 (2). https://doi.org/10.1088/1741-2552/aafa05.

Sinderby, C., Lindström, L., Grassino, A.E., 1995. Automatic assessment of electromyogram qualityitle. Journal of Applied Physiology 79 (5), 1803–1815. https://doi.org/10.1152/jappl.1995.79.5.1803.

Spinelli, E., et al., 2016. A simple and reproducible capacitive electrode. Medical Engineering and Physics 38 (3), 286–289. https://doi.org/10.1016/j.medengphy.2015.12.006.

Spinelli, E.M., Mayosky, M.A., 2005. Two-electrode biopotential measurements: Power line interference analysis. IEEE Transactions on Biomedical Engineering 52 (8), 1436–1442. https://doi.org/10.1109/TBME.2005.851488.

Takada, H., 2012. Electromyography: New developments, procedures and applications, 1st edn. Nova Biomedical Books, USA.

De Talhouet, H., Webster, J.G., 1996. The origin of skin-stretch-caused motion artifacts under electrodes. Physiological Measurement 17 (2), 1–8. https://doi.org/10.1088/0967-3334/17/2/003.

Tam, H.W., Webster, J.G., 1977. Minimizing Electrode Motion Artifact by Skin Abrasion. IEEE Transactions on Biomedical Engineering 24 (2), 134–139. https://doi.org/10.1109/TBME.1977.326117.

Texas Instruments, 1995. *Understanding data converters, SLAA013, Mixed-Signal Products*. Application Reports.

Turner, I.N., et al., 1995. Noise coherence in closely-spaced electrodes: The implications for spatial averaged EGG recordings. Journal of Medical Engineering and Technology 19 (5), 158–161. https://doi.org/10.3109/03091909509009987.

Webster, J.G., 1984. Reducing Motion Artifacts and Interference in Biopotential Recording. IEEE Transactions on Biomedical Engineering 31 (12), 823–826. https://doi.org/10.1109/TBME.1984.325244.

Webster, J.G., 2013. Medical Instrumentation-Application and Design. John Wiley & Sons. https://doi.org/10.1097/00004669-197807000-00017.

Winder, S., 2002. Analog and digital filter design. Elsevier Inc.

Winter, B.B., Webster, J.G., 1983a. Reduction of Interference Due to Common Mode Voltage in Biopotential Amplifiers. IEEE Transactions on Biomedical Engineering 30 (1), 58–62. https://doi.org/10.1109/TBME.1983.325167.

Winter, B.B., Webster, J.G., 1983b. Driven-Right-Leg Circuit Design. IEEE Transactions on Biomedical Engineering 30 (1), 62–66. https://doi.org/10.1109/TBME.1983.325168.

Yousef, H., Alhajj, M., Sharma, S., 2019. Anatomy, skin (integument), epidermis. StatPearls Publishing, Available at: https://www.ncbi.nlm.nih.gov/books/NBK470464/.

Zhao, Z., Zhang, Y., 2018. SQI quality evaluation mechanism of single-lead ECG signal based on simple heuristic fusion and fuzzy comprehensive evaluation. Frontiers in Physiology 9 (727), 1–13. https://doi.org/10.3389/fphys.2018.00727.

Zucca, A., et al., 2015. Tattoo Conductive Polymer Nanosheets for Skin-Contact Applications. Advanced Healthcare Materials 4 (7), 983–990. https://doi.org/10.1002/adhm.201400761.

Prof. Roberto Merletti graduated in Electronics Engineering from Politecnico di Torino, Italy, and obtained his M.Sc. and PhD in Biomedical Engineering from the The Ohio State University. He has been Associate Professor of Biomedical Engineering at Boston University were he was also Research Associate at the NeuroMuscular Research Center. He has been Full Professor of Biomedical Engineering at Politecnico di Torino where he established, in 1996, the Laboratory for Engineering of the Neuromuscular System (LISiN) of which he has been Director up to 2015. He has trained at LISIN more than 70 researcher (15 doctoral students) from various countries. His research activity covered basic investigation of sEMG, applications in prevention, rehabilitation, ergonomics, sport. This activity led to over 200 peer reviewed publications and four textbooks. He is Senior Member of IEEE, Fellow of ISEK, and member of the Editorial Board of three international journals. His e-mail is roberto.merletti@formerfaculty.polito.it and his personal web site is www.robertomerletti.it which has a strong teaching connotation.

Giacinto Luigi Cerone obtained the M.Sc. degree in Biomedical Engineering in 2014 and the PhD in Bioengineering and Medical-Surgical Sciences summa cum laude in 2019 from Politecnico di Torino, Torino, Italy. Since 2013, he is a fellow of the Laboratory for Engineering of the Neuromuscular System at Politecnico di Torino. His main research interests concern the hardware, firmware, software design, and certification of biomedical instrumentation for High-Density surface EMG signals acquisition and Neuromuscular Electrical Stimulation.